IOWA STATE UNIVERSITY
Digital Repository

2009

Investigations into the fate and behavior of selected inorganic compounds during biomass gasification

Patrick Marshall Meehan
Iowa State University

Follow this and additional works at: http://lib.dr.iastate.edu/etd

Part of the Mechanical Engineering Commons

Recommended Citation

Investigations into the fate and behavior of selected inorganic compounds during biomass gasification

by

Patrick Marshall Meehan

A thesis submitted to the graduate faculty

in partial fulfillment of the requirements for the degree of

MASTER OF SCIENCE

Major: Mechanical Engineering

Program of Study Committee:
Robert C. Brown, Major Professor
Theodore J. Heindel
D. Raj Raman

Iowa State University

Ames, Iowa

2009

TABLE OF CONTENTS

LIST OF FIGURES

v

LIST OF TABLES

ABSTRACT

Two sets of gasification experiments were performed in an effort to understand the fate of biomass nutrients and the effects of feedstock potassium on carbon conversion during gasification. The purpose of this research was to develop a comprehensive understanding of the issues of sustainability and efficiency facing biomass gasification. The results of these studies are described in detail within this thesis.

The first study evaluated the fate of biomass nutrients in an integrated system of biomass production and gasification. Eight plots of switchgrass were grown and harvested for use in this study. Four plots were fertilized with 65 kg ha^{-1} of nitrogen (N) and four plots were not fertilized. Three essential biomass nutrients N, phosphorus (P), and potassium (K) as well as carbon (C) were individually tracked through a fluidized bed gasifier and subsequent gas clean up equipment. Mass balances were performed on each element to determine the percentage of that element that was able to be accounted for and the percentage that was able to be recovered in a form suitable for use as a soil amendment.

The percentage of C recovered in a form suitable for field sequestration was independent of fertilizer N input and represented 13±1% (mean±SD) of switchgrass C. Recovery of N in a form suitable for soil amendment was 55±7% of switchgrass N and was also independent of fertilizer N. The percentages of P and K recovered in forms suitable for soil amendment were both higher for the fertilized treatment of switchgrass than the unfertilized treatment. Recovery of P in a form suitable for soil amendment was 73±21% for the unfertilized treatment and 104±24% for the fertilized treatment. Likewise for K, recovery percentages for unfertilized and fertilized treatments were 61±9% and 71±9% respectively.

The second study investigated the role of potassium and reaction temperature on carbon conversion during air blown fluidized bed gasification. To accomplish this, corn fiber, a low potassium biomass, was doped with varying amounts of potassium chloride and gasified at different temperatures. A statistical design of experiments consisting of 12 experiments was completed. Mass balances were performed and carbon conversion was determined. The results were used to generate a statistical model that was subsequently analyzed.

The model predicted maximum carbon conversion for a feedstock potassium content of 1.85 wt% K and a bed temperature of 817 °C. The model also showed that carbon conversion was affected more by changes in bed temperature than changes in feedstock potassium content over the range of operating conditions used in this study. The observation that carbon conversion decreased above 817 °C was surprising but may be the result of increased volatilization of K, which would decrease the amount of K in contact with gasifying biomass. The apparently negligible effect of feedstock K on carbon conversion could be due to the potency of K as a gasification catalyst at concentrations as low as 0.3 wt%.

CHAPTER 1. GENERAL INTRODUCTION

Introduction

Over the past decade it has become increasingly evident that clean, renewable energy must be developed. Gasification represents a versatile solution to meet this energy demand. The main product of gasification is producer gas (a mixture of N_2, carbon monoxide (CO), carbon dioxide (CO_2), hydrogen (H_2), methane (CH_4), and short-chain hydrocarbon gases) that can be upgraded to liquid transportation fuels and high value chemicals, or simply used as a fuel to generate heat and electricity. Biomass represents an invaluable gasification feedstock. Not only is it renewable, but it is also available in the quantities required to compete in today's market [1]. However, the success of biomass gasification in the context of this development depends on two things: sustainability and efficiency.

Gasification of biomass is also an attractive means for energy and fuel production due to its efficiency and its potential to recover biomass nutrients [2]. Research by Lehmann et al. [3] indicate that char produced from thermochemical processes can be sequestered in the soil allowing the field to act as a long term carbon sink. Research by Day et al. [4] describe a process for capture of biomass nutrients in char that can later be applied to the field. This recovery of nutrients is essential in a biomass based energy platform. Perlack et al. [1] show that the harvest of biomass for energy production on a national scale directly causes the removal of thousands of tons of biomass nutrients from the soil. This wholesale removal of vital plant nutrients represents a challenge to the sustainable production of feedstock and a very large cost to feedstock producers.

Anex et al. [2] show that biomass nutrients entering a gasifier concentrate in the char or are incorporated in the gas stream during gasification. By understanding what happens to the nutrients during gasification, nutrients in both of these streams could potentially be recovered and returned to the crop fields from which biomass feedstocks were generated, thereby closing the nutrient cycle and making the process more sustainable.

To be competitive with fossil fuels, biomass conversion processes must be highly energy efficient. Extensive catalysis research has been performed on both primary (in the gasifier) and secondary (downstream of the gasifier) reactors to increase the gasification efficiency [5]. A simpler and less costly method would be to use the inherent properties of the biomass to increase the efficiency of the gasification process. Different types of biomass contain different amounts of alkali and alkali earth metals such as sodium (Na), K, calcium (Ca), and magnesium (Mg) [6]. Historically the presence of alkali metals during gasification has been viewed as detrimental because they can cause fouling and damage to boiler tubes, turbine blades, and gas clean up equipment [7]. However, more recent research by Brown et al., Godavarty et al., and Sjostrom et al. [8-10] suggest that alkali metals can increase process efficiency. These studies show that alkali increases gasification rate, increases gas production, and decreases char production. It follows then that alkali metals may increase the efficiency of biomass gasification. If correctly understood and implemented, biomass could be selected for gasification based upon alkali metal content thereby simplifying processing equipment and saving money.

This research investigates the potential to increase the sustainability of the bioeconomy by recovering biomass nutrients during gasification. It also explores the effects

of biomass potassium content and gasifier bed temperature on carbon conversion in an effort to increase the efficiency of biomass gasification.

Thesis Organization

This thesis has been prepared from two manuscript papers. The first is entitled *Switchgrass Gasification: Mass Balance and Nutrient Recovery*. This paper focuses on nutrient recycling of the essential plant nutrients N, P, and K as well as C during gasification. In this research, N, P, K, and C were tracked and accounted for through the system to determine the feasibility of recycling these nutrients in the form of char and ammonia, back to the field as soil amendments.

The second paper is entitled *Carbon Conversion during Gasification as a Function of Potassium Content of Biomass*. This paper investigates role of feedstock potassium content and bed temperature on carbon conversion during biomass gasification. In this research, different feedstock potassium contents were simulated using corn fiber and a potassium chloride and water (KCl/H_2O) solution. The corn fiber was gasified at different temperatures to determine the effects of these two variables on carbon conversion. A statistical model was generated from the data and conclusions based on both the raw data and the model are discussed.

These papers are preceded by a background chapter that reviews the technical literature on topics relevant to the study of inorganic compounds during biomass gasification. The thesis concludes with a discussion summary of the results of the two papers and provides recommendations for future research.

CHAPTER 2. REVIEW OF LITERATURE

Gasification

Gasification is defined by Brown [11] as "the high temperature conversion of solid, carbonaceous fuels into flammable gas mixtures." Unlike pyrolysis in which the reactor environment is inert, or combustion in which oxygen concentration is present at stoichiometric conditions, gasification occurs in a hypostoichiometric environment. The oxidizer used for gasification is typically air, oxygen (O_2), steam, CO_2 or any combination of this group. To quantify the amount of oxygen used, the equivalence ratio, shown in Equation 1, is calculated.

$$ER = \frac{(M_{O_2}/M_{Fuel})_{Actual}}{(M_{O_2}/M_{Fuel})_{Stoichiometric}} \qquad (1)$$

where: ER is equivalence ratio
M_{O2} is the amount of oxygen introduced into the gasifier (kg)
M_{Fuel} is the mass of fuel introduced into the system (kg)

Typically equivalence ratios range from 0.21 to 0.49 depending on the desired products as well as the reactor [12]. There are many different gasifier styles including updraft, downdraft, fluidized bed, circulating fluidized bed, and entrained flow [11]. The reactor used in this study was an air blown fluidized bed gasifier, a schematic of which is shown in Figure 1.
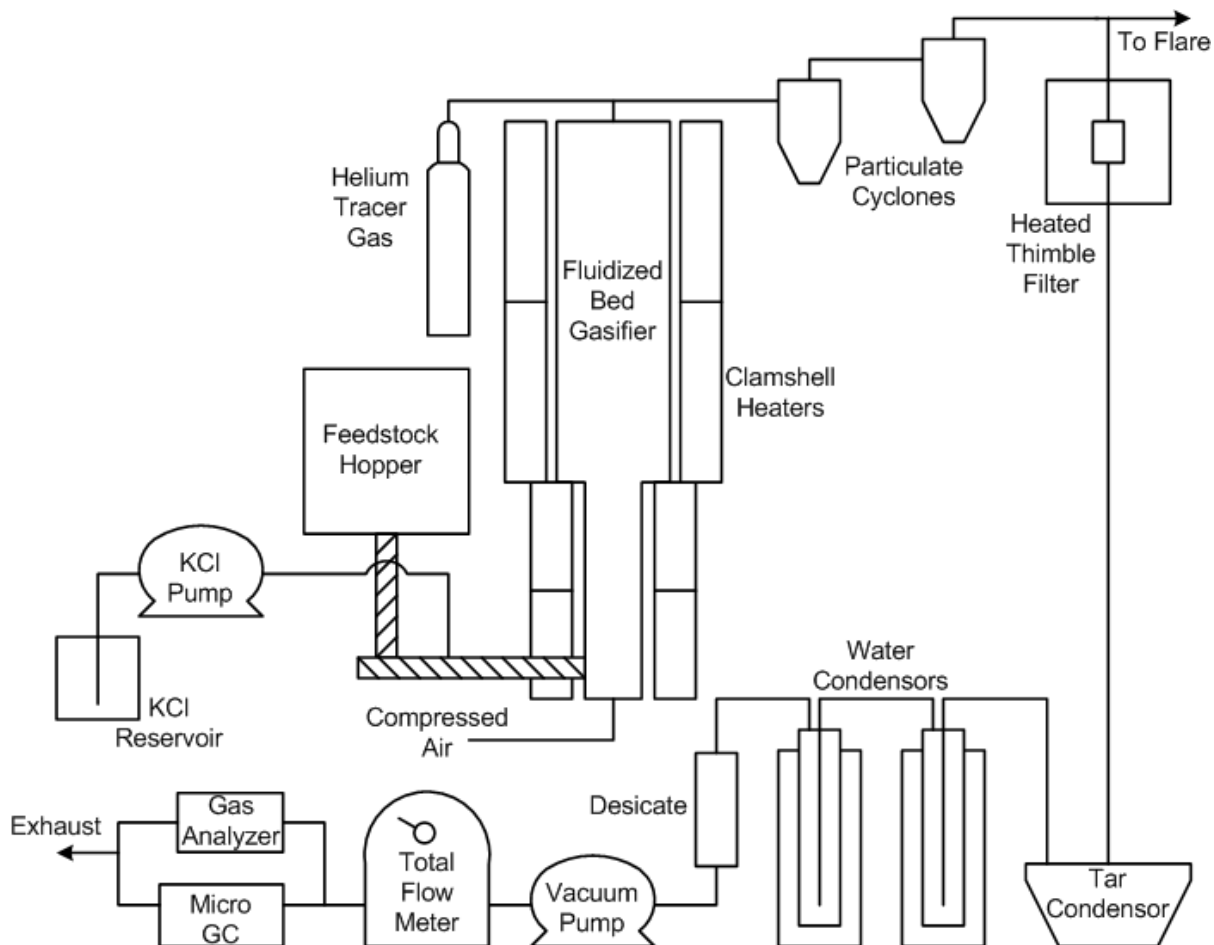
Figure 1: Schematic diagram of the air blown fluidized bed gasifier used in this research

Gasification transforms fuel and oxidizer into a mixture of char, tar, and gas. Fuels can be any carbonaceous material such as coal, herbaceous or woody biomass, or even refuse. Char is formed when the feedstock devolatilizes leaving a carbon based solid that can then be reacted further or entrained in the gas stream and elutriated from the reactor. Depending on the nature of the feedstock and the operating conditions present in the reactor, char yields vary from about 5 to 15% of the total mass of the fuel. Typically about 34 to

6

57% of the char is carbon, 1 to 5% is a mixture of N, O, H, and sulfur (S), and the remainder is ash, a mixture of inorganic constituents including K, Na, P, and silicone (Si) [13]. An analysis of ash compositions of six different types of biomass is shown in Table 1 [6]. Ash quantity and composition varies widely depending on the type of fuel with coal typically having higher ash content than biomass [7]. The major alkali metal found in coal ash is Na while the alkali metal in biomass ash is primarily K [7].

Table 1: Ash composition of 6 types of biomass[1] [6]

Plant organ	Ash	N	C	Al	Ca	Cl	Fe	K	Mg	Na	P	S	Si	Si/K	Ca/K
Leaves															
Arundo d.	113	15.7	430	461	6167	6986	308	5080	2182	159	803	3511	17232	3.4	1.2
Cynara c.	117	9.6	417	1781	27802	13143	655	4711	1876	11942	1459	3760	4267	0.9	6.1
Miscanthus s.	62	6.3	431	595	5262	6701	324	3265	1291	193	396	867	16666	5.1	1.6
Panicum v. 20	76	7.4	423	543	6922	9490	319	2126	2706	326	774	991	15745	8.0	3.6
Panicum v. 80	70	8.4	428	435	8182	3617	283	1504	2626	317	578	1048	15036	10.1	5.5
Fibre s.	81	13.4	424	483	9245	4737	236	8805	3086	195	1246	1105	19736	2.3	1.1
Sweet s.	82	13.5	425	328	8359	3741	186	11661	2805	189	1273	1099	14858	1.3	0.7
Mean	86	10.6	425	661	10277	6916	330	5307	2367	1903	933	1769	14791	4.4	2.8
Stems															
Arundo d.	32	5.2	431	196	968	5608	102	5609	1027	130	320	932	6223	1.1	0.2
Cynara c.	68	3.0	401	150	12190	18171	79	6467	766	12807	1363	1740	889	0.2	2.1
Miscanthus s.	19	1.6	439	143	1730	7406	61	3588	857	153	154	337	4531	1.3	0.5
Panicum v. 20	26	3.0	435	137	1097	13798	86	3555	1020	870	404	464	5345	1.5	0.3
Panicum v. 80	23	3.3	440	111	1197	4944	83	2628	1171	870	248	443	5301	2.1	0.5
Fibre s.	41	2.6	409	114	2643	6398	79	12577	1903	193	702	817	5345	0.4	0.2
Sweet s.	50	4.4	408	152	3446	7199	112	12991	2079	195	804	681	7013	0.5	0.3
Mean	37	3.3	423	143	3325	9075	86	6774	1260	2174	571	773	4950	1.0	0.6
Reproductive organs															
Cynara c.	67	14.3	444	106	9960	9863	71	19325	1815	1340	2427	1708	474	0.0	0.5
Fibre s.	47	13.1	434	242	1824	6252	141	5587	2451	192	2150	1084	10671	2.0	0.3
Sweet s.	58	14.1	424	218	2417	5129	159	7125	2895	171	2620	1000	14321	2.0	0.3
Mean	57	13.8	434	189	4734	7081	124	10679	2387	567	2399	1264	8489	1.4	0.4

Tar is a viscous dark brown to black liquid at standard conditions and can account for up to 10% of the total mass of the fuel [11]. It is commonly defined as "all organic contaminants with a molecular weight larger than benzene." [14] Historically tar has been a problem for gasification because tar is difficult to remove and represents a source of inefficiency. As gasification temperature increases, primary (single ring aromatic

[1]Ash, N, and C are expressed as g kg^{-1} while other elements are expressed as mg kg^{-1}

hydrocarbons) and secondary (double ring aromatic hydrocarbons) tar production decreases but a larger amount of tertiary (triple ring aromatic hydrocarbons) and larger tars are produced [14]. Increasing the equivalence ratio can also decrease tar production due to higher oxygen concentration in the reactor [14]. Formation of tertiary and higher tars is seen at longer residence times while tars tend to have lower molecular weight at shorter residence times [14].

Gas is the major product of gasification. When pure O_2 is used as an oxidizer, the resulting gas is called syngas. When air is used, the term producer gas defines the nitrogen-rich product. Producer gas always contains the same major constituents: N_2, CO, CO_2, H_2, and CH_4. However, depending on what fuel, oxidizer, equivalence ratio, temperature, and reactor geometry are chosen, the composition of the producer gas changes. Typically additional short-chain hydrocarbons including acetylene (C_2H_2), ethylene (C_2H_4), ethane (C_2H_6), and propane (C_3H_8) are also formed in small amounts. The producer gas accounts for about 70 to 90% of the total mass of the fuel fed into the gasifier.

Carbon Conversion

Carbon conversion is an important measure of the effectiveness of gasification. It is defined as the percentage of carbon in the solid feedstock that is converted into gaseous product. It can be calculated from the amount of carbon remaining as char using Equation 2.

$$CC = \frac{M_{FC} - M_{CC}}{M_{FC}} \qquad (2)$$

where: CC is carbon conversion (%)
            M_{CC} is the mass of carbon in the char (kg)
            M_{FC} is the mass of carbon in the feedstock (kg)

Although tar can also be a source of carbon loss to the gas stream, this method assumes that all volatilized material counts as "gasified product." Therefore, it is normally desirable to minimize the production of char to increase the carbon conversion. There are many ways which carbon conversion can be increased. Decreasing biomass particle size, decreasing superficial gas velocity, increasing temperature, and increasing equivalence ratio are all ways to decrease char production and therefore increase carbon conversion and have been investigated [15]. However, this research focuses on using alkali metals naturally present in biomass as a means of increasing carbon conversion.

Alkali Metal Effects in Gasification

Alkali Metals

While carbon conversion is well understood within the context of parameters such as temperature and equivalence ratio, it is also linked to more enigmatic factors such as feedstock alkali metal content. Alkali metals form the first group of the periodic table and include lithium (Li), Na, K, rubidium (Rb), cesium (Cs), and francium (Fr). Due to their reactive characteristics, alkali metals in their elemental state rarely occur naturally. As biomass is concerned Na and K are both important plant nutrients. However since K has been at the center of this research it will also be the major focus of this review.

The Benefits of Alkali

The majority of literature regarding alkali as it relates to power generation and fuel production focuses on coal rather than biomass and combustion rather than gasification [7, 16]. Brown et al. and Godavarty et al. [8, 9] both state that in general, as coal rank decreases (typically meaning higher alkali metal content) gasification rate increases. Doping coal with alkali has also been studied. Brown et al. [8] show that a 1 wt% increase in potassium causes a one order of magnitude increase in coal gasification rate. Brown et al. [8] conclude that alkali metal salts act as productive catalysts in the promotion of coal gasification, but are often too expensive to use for this purpose. To avoid the high cost of these alkali catalysts, co-gasification of coal with biomass or biomass ash has been attempted [8, 10]. These studies conclude that biomass alkali contributes to decreased char production and increased gasification rates in coal gasification. This research substantiates the hypothesis that biomass alkali increases energy conversion efficiency in biomass gasification.

In addition to increased carbon conversion, there are other benefits to understanding the role of alkali in biomass gasification. Garcia-Garcia et al. [17] show that coal with high potassium content reduces NO_x emissions better than coal with low potassium content. Similar favorable effects are likely with biomass. Alkali could also help promote specific types of reactions. For example, because methane formation is exothermic it favors low reactor temperatures. However at these lower temperatures, gasification rate is slower and the energy conversion efficiency of the process is lower. By using alkali as a catalyst, gasification could potentially be performed at lower temperatures allowing an increase in methane production without a decrease in energy conversion efficiency [8]. The

development of hot gas clean up technologies could also benefit from a better understanding

alkali metals' behavior in gasification [18]. For example, a portion of biomass alkali

vaporizes in gasification conditions and forms sub-micron fumes that cannot be captured by

conventional equipment such as cyclones and even many types of fabric filters [7]. So

although alkali can be of great benefit to the field of gasification, it can also prove

detrimental to many types of equipment.

Deleterious Effects of Alkali

The gas turbine is a prominent example of equipment that is adversely affected by

alkali. The maximum amount of gas phase alkali acceptable for turbine operation is ~ 0.1

ppmw [13]. However, gasification of biomass has been shown to produce 1 to 10 ppmw of

gas phase alkali vapor in the producer gas stream [19]. The pressure and temperature drop

across a turbine causes this alkali vapor to nucleate, condense, and deposit on the turbine

blades [7, 20]. Over time hot corrosion will destroy a turbine blade [13]. Alkali can also

foul boiler tubes in steam boilers by condensation of a sticky film that promotes deposition of

particulate matter [8, 13, 18]. In fluidized bed research, such as that which was performed

for this research, agglomeration due to the presence of alkali is commonly observed [13, 21].

The major alkali metal responsible for this agglomeration is potassium [13, 20].

Potassium in Biomass Gasification

Biomass alkali is typically composed of plant nutrients and varies widely depending

on the production location and species of plant [18]. Potassium is the major alkali metal

constituent in biomass as shown in Table 1 [6]. It is an essential plant macronutrient and

typically occurs in concentrations of < 5 wt% [13]. Potassium is normally found in water

solutions located inside plant vacuoles rather than being part of structural components [7]. It

can also be found active in various enzymes [7]. Because of these locations, K most likely

volatilizes only as inorganic forms such as chlorides, oxides, free metal or fine powders

unlike other alkali metals which likely volatilize as both organic and inorganic compounds

[7]. Relatively high chlorine content in biomass aids K mobilization but the high oxygen

content of the fuel creates an oxidizing environment which tends to repress the release of K

in its metal form [7]. In addition, larger biomass particle size means that there is a greater

chance for sequestration of alkali, including K, as it migrates outward through the particle

[7].

In contrast to biomass, the major alkali component of coal is Na [7]. Sodium and

other types of alkali metal are normally found in micron sized mineral or salt inclusions such

as carboxylate or phenolate organic functional groups [7, 18]. These clays can act to

sequester the alkali during heating, lowering the available amount and ease of vaporization

[7, 16]. The total amount of alkali in coal ranges from 0.01 to 1.0 wt% [7]. However,

although there may be less total alkali in coal than biomass, coal is traditionally pulverized

and therefore has a smaller particle size than biomass when introduced into a gasifier causing

it to react hotter, faster, and more violently than the biomass. This leads to a greater potential

for alkali vapor release [7].

Although the majority of literature regarding alkali deals with combustion, some

parallels can be drawn between alkali behavior during combustion and gasification. During

combustion, Dayton et al. [18] observe that K is typically released as salts in the form of

chlorides, hydroxides, or sulfates as well as K^+. Of these, KCl is the most common species [18]. The release of this alkali can be affected by gas concentration. Matsuoka et al. [21] find that the high concentrations of CO in gasification enhance mineral decomposition leading to a greater vaporization of metallic K.

Regardless of feedstock, K content in the gas stream begins climbing around 700 °C [19]. This is in part because K remains fixed at lower temperatures due to the formation of leucite ($K[AlSi_2O_6]$) [22]. This means that for a significant liberation of K to occur bed temperatures need to exceed 700 °C. Also, Kitsuka et al. [23] show that forced gas flow causes a larger volatilization of K which suggests possible correlations between superficial fluidizing gas velocity and K volatilization. Furthermore, French et al. and Thompson et al. [7, 16] observe an increase in gas phase K in reducing environments. However, minerals shielded from alkali loss until rapid cooling takes place will retain the majority of their alkali [16]. For example, in the extreme temperatures of the reducing surroundings of a combustor flame zone or gasifier distributor plate, alkali is probably a metal vapor [7]. The addition of limestone to the bed also increases gas phase K [16, 22].

Although some inorganic species such as Ca tend to form aluminosilicates, Matusuoka et al. [21] show that the primary pathway for the release of K during gasification is vaporization. The amount of K vaporization differs between equilibrium calculations and experimentation as well as between research groups. Equilibrium models from Thompson et al. [16] predict 10 to 15% gas phase alkali and 85 to 90% liquid phase alkali for equivalence ratios ranging from 0.25 to 0.35 and temperatures over the range of 700 to 900 °C. However, experiments performed find no liquid phase alkali [16, 20]. Turn et al. [13]

conclude that the total amount of alkali vapor released is lower in experimental work than in equilibrium modeling, predicting that KCl will be the primary form of alkali vapor released during gasification and that K vapor will increase as Cl increases. It should not be discounted, though, that this increase could be a result of increasing K concentration as Cl concentration increases due to KCl in the biomass.

The accumulation and retention of K during gasification is of acute importance to this thesis as K is a major focus of both studies. Turn et al. [13] show that 40 to 80 wt% of the K fed into a gasifier is retained in the bed while the remainder is filtered out of the gas stream with the char. However, Mojtahedi et al. [24] found 97% alkali in the cyclone catch, 6.7% in post cyclone filtration, and 1.2% as a vapor in the gas stream while tracking combined alkali (K and Na). The argument that the majority of K is filtered out of the gas stream is backed by independent research from French et al. [7] They state that K remains as a vapor in conditions exceeding 950 °C such as is sometimes seen inside a gasifier [7]. Thompson et al. [16] find that the majority of alkali vapor condenses in the range of 550 to 600 °C. Condensation of alkali vapor has been known to occur on char, and scanning electron microscopy has been used to photograph bright spots on char that are suspected to be alkali deposits [7, 21].

Bed loading of K is also important as the concentration of K in the bed will likely impact the energy conversion efficiency if K is in fact a successful biomass gasification promoter. Gabra et al. [20] show 12% retention of combined alkali in the bed after 1.4 hrs and 4% retention after 12 hrs. As the length of the experiment increases, the amount of K retained in the bed decreases, suggesting that in fluidized bed gasification K concentration in

the bed increases and then decreases to eventually reach a steady state. One point that multiple researchers have agreed upon is that bed K loading is proportional to feedstock K concentration, indicating that the bed is an important storage place for the K [13, 19].

The literature described in this review adds validity to this thesis research. First, the literature shows that K increases gasification rate, increases gas production, and decreases char production. Second, the literature shows that K resides in the bed during gasification. These two conclusions strongly suggest that favorable catalytic effects of K on carbon conversion during fluidized bed gasification of biomass are likely.

Fluidized Bed Reactors

An air blown fluidized bed gasifier was used in these studies. Fluidized beds are used for many applications including drying, pyrolysis, gasification, and combustion [25]. The bed consists of solid particles whose properties depend on the application and desired type of fluidizations. In the case of this research, a mixture of silica sand and crushed limestone was used. Gas enters the bottom of the reactor through a distribution system which can be a porous plate, nozzle system, perforated plate, or other configuration. As the amount of gas rising through the particles increases, the friction force due to the gas flowing past the particles increases. Eventually the weight of the particles is balanced by the force of friction, and a phenomenon known as minimum fluidization occurs. This phenomenon represents a type of equilibrium in which the particles are suspended by the gas flow but relatively little mixing is occurring. As the gas flow is further increased, the particles begin to move, mix, and turn. Bubbles begin to form as a result of the excess gas flow and rise to the top of the

bed causing a state similar to boiling. At this state of full fluidization, the bed can be considered very well mixed with high heat and mass transfer rates, properties that are very attractive from a gasification standpoint.

The fluidized bed gasifier is separated into a plenum, bed, splash zone, and freeboard. The plenum is located below the bed and serves to preheat and diffuse the incoming gas stream before it enters the reactor. The bed, as described above, can be fed with fuel from virtually any location. In the case of this research, biomass is fed in the side of the reactor at the bottom of the bed with a fast moving auger. As it comes in contact with the hot bed material, the moisture and volatile matter within the biomass is driven off, leaving char. The splash zone, located above the bed, is formed as a result of the violent mixing that occurs in the bed. It typically contains bed material, biomass, and char from popping bubbles and splashing occurring in the bed. The freeboard is a longer section of the reactor located above the splash zone. As is the case with this reactor, it is typically a larger diameter than the bed. This expansion serves to slow the exiting gases, promoting further reactions as well as the disengagement of particles entrained in the gas stream. For more information about fluidized beds please refer to Basu [25].

CHAPTER 3. SWITCHGRASS GASIFICATION: MASS BALANCE AND NUTRIENT RECOVERY

A paper to be submitted to *Biotechnology for Biofuels*

Patrick M. Meehan[1], Andrew H. Heggenstaller[2], Samuel T. Jones[3], Robert P. Anex[4], and Robert C. Brown[5]

[1]Primary responsibility for gasification, developed nutrient tracking techniques, and drafted the manuscript. [2]Helped conceive and design the study, managed switchgrass production, assisted with gasification, performed statistical analysis, organized chemical analysis, and edited manuscript. [3]Supervised gasification, and reviewed and commented on the manuscript. [4]Helped conceive and design the study, and reviewed and commented on the manuscript. [5]Helped conceive and design the study, and reviewed and commented on the manuscript.

Abstract

Background: Thermochemical conversion of biomass operated in a manner to recover key fertilizer nutrients could allow for continuous nutrient cycling between crop fields and biorefineries, thereby closing nutrient cycles and reducing the energetic and economic costs of bioenergy production. The objective of this study was to systematically track flows and recovery potential for major plant nutrients during the gasification of switchgrass biomass that had been produced with no or low (65 kg ha^{-1}) fertilizer nitrogen inputs. Three essential plant nutrients (nitrogen, phosphorus, and potassium), as well as carbon were individually tracked throughout the system, and the quantity of each that could be recovered was determined.

Results: On average, the overall mass balances across the gasifier for all 8 experiments closed to 93±12% (mean±SD) suggesting that experimental methods were

reliable in tracking mass and nutrient flows. Carbon (C) and phosphorus (P) mass balances closed to 90±12% and 101±25%, respectively, indicating that these elements were successfully tracked throughout the process of gasification. In contrast, the nitrogen (N) and potassium (K) mass balances closed only to 56±8% and 71±10%, respectively, indicating systematic loss of these elements during gasification in a form that was not quantified in this study. The percentage of C recovered in a form suitable for field sequestration was independent of fertilizer nitrogen input and represented 13±1% of switchgrass C. Recovery of N in a form suitable for soil amendment was 55±7% of switchgrass N and was also independent of fertilizer nitrogen. The percentage of P and K recovered in forms suitable for soil amendment were both higher for the fertilized treatment of switchgrass than the unfertilized treatment. Recovery of P in a form suitable for soil amendment was 73±21% for the unfertilized treatment and 104±24% for the fertilized treatment. For K, recovery percentages for unfertilized and fertilized treatments were 61±9% and 71±9% respectively.

Conclusion: Mass balances on an overall basis and an element-specific basis for C, N, P, and K were completed for the gasification of unfertilized and fertilized treatments of switchgrass to determine the feasibility of recovering biomass nutrients during gasification. Element-specific mass balances for C and P show that both elements can be well accounted for in gasification. However, element-specific mass balances on N and K closed to less than 100% with statistical significance. N-specific mass balances could likely be increased by measuring other nitrogen compounds in the gas stream such as hydrogen cyanide (HCN), although this would not necessarily increase the amount of recoverable N that could be returned to the field. K-specific mass balances could likely be increased by utilizing a barrier

filter to capture gas entrained K passing through the cyclones. This approach could increase amount of recovered K from 66% of the total amount of K in the switchgrass to 77%. On average 13% of switchgrass C was recovered for sequestration and 55% of N, 89% of P, and 66% of K were recovered in a form suitable to be used as soil amendments.

Background

Thermochemical conversion of biomass is an attractive means for energy and fuel production due to its efficiency and its potential to recover biomass nutrients [2]. Research by Lehmann et al. [3] indicate that char produced from thermochemical processes can be sequestered in the soil allowing the field to act as a long term carbon sink. Additional research by Day et al. [4] describe a process for capture of biomass nutrients in char that can later be applied to the field. This recovery of nutrients is essential in a biomass based energy platform. Perlack et al. [1] show that the harvest of biomass for energy production on a national scale directly causes the removal of thousands of tons of biomass nutrients from the soil. This wholesale removal of vital plant nutrients represents a challenge to the sustainable production of feedstock and a very large cost to feedstock producers.

Integrated lignocellulosic biofuel production facilities envisioned for the future will tend to concentrate these vital plant nutrients in the waste and by-products of thermochemical conversion. Even for biochemical fuel production processes, thermochemical conversion is expected to produce the heat and power for the biochemical processes, while residue from the biochemical process will provide the fuel for the thermochemical process [26]. In such a scenario, nutrients that enter the conversion process in the lignocellulosic biomass are

assumed to concentrate in the fly ash (e.g., P and K) or be incorporated in the gas stream during gasification [2]. Nutrients in both of these streams can potentially be recovered and returned to the fields where the biomass feedstocks were grown. However, technologies for nutrient recovery are not commercially available today. In order to efficiently recover these critical plant nutrients from the biofuel production process, we must know their physical and chemical forms and locations. This paper is the first report on the systematic tracking of major plant nutrients during gasification of switchgrass (*Panicum virgatum* L.), a widely promoted energy crop.

Methods

Feedstock Production

Switchgrass (var. 'Cave-In-Rock') was produced at the Iowa State University (ISU) Agronomy and Agricultural Engineering Research Farm in Boone County, Iowa, USA ($42^o0'$ $40''$N; $93^o44'46''$W). Soils at the experimental site were classified as Canisteo silty clay loam (fine-loamy, mixed, superactive, calcareous, mesic, Typic Endoaquolls), Webster silty clay loam (fine-loamy, mixed, superactive, mesic, Typic Endoaquolls), and Clarion silty clay loam (fine-loamy, mixed, superactive, mesic, Typic Hapludolls). Four replicated switchgrass plots were established in 2003 in a field that had been managed as a corn-soybean rotation. Beginning in 2006, switchgrass plots were treated with either 0 or 65 kg N ha^{-1} (as NH_4NO_3) in May as a randomized complete block design, and all aboveground biomass was harvested and weighed following a killing frost in mid-October. Subsamples were collected at the time of harvest for determination of moisture and nutrient content. In October 2007, harvested

biomass was air-dried for two weeks, ground to 6 mm in a tub grinder, and then dried for approximately one more week in a large forced air oven at 140 °F. Following grinding and drying, the switchgrass was weighed and stored in sealed plastic bins to await gasification.

Gasification and Nutrient Tracking

Ground, dried switchgrass was gasified in spring 2008 using a fluidized bed gasifier shown in Figure 2. Each of the eight bins of switchgrass was gasified on a separate day over the course of approximately three weeks. The gasification vessel consists of three sections: plenum, fluidized bed, and freeboard. The plenum, in conjunction with a distributor plate, serves to evenly distribute air flow to ensure smooth fluidization. The incoming air stream was metered by a 0 to 150 slpm Alicat mass flow controller (Alicat Scientific Tucson, AZ) and heated to 400 °C by a Watlow coil heater (Watlow, St. Louis, MO). The bed is 10 cm in diameter and filled with media consisting of a mixture of 70 wt% 200-300 μm silica sand, and 30 wt% ground limestone, totaling 2.2 kg. Bed media was sampled before and after each of the eight experiments to assess possible retention of nutrients and carbon in the gasifier. Bed media removed with each sample was replaced prior to the following experiment to maintain a constant bed mass throughout the course of the study. Ground switchgrass was injected into the bed via an auger system directly above the distributor plate. The freeboard has a diameter of 15 cm. This increase in diameter between the bed and freeboard slows the gas velocity causing disengagement of particles from the gas stream. For more information on the gasifier used in this study please refer to Emsick [27].
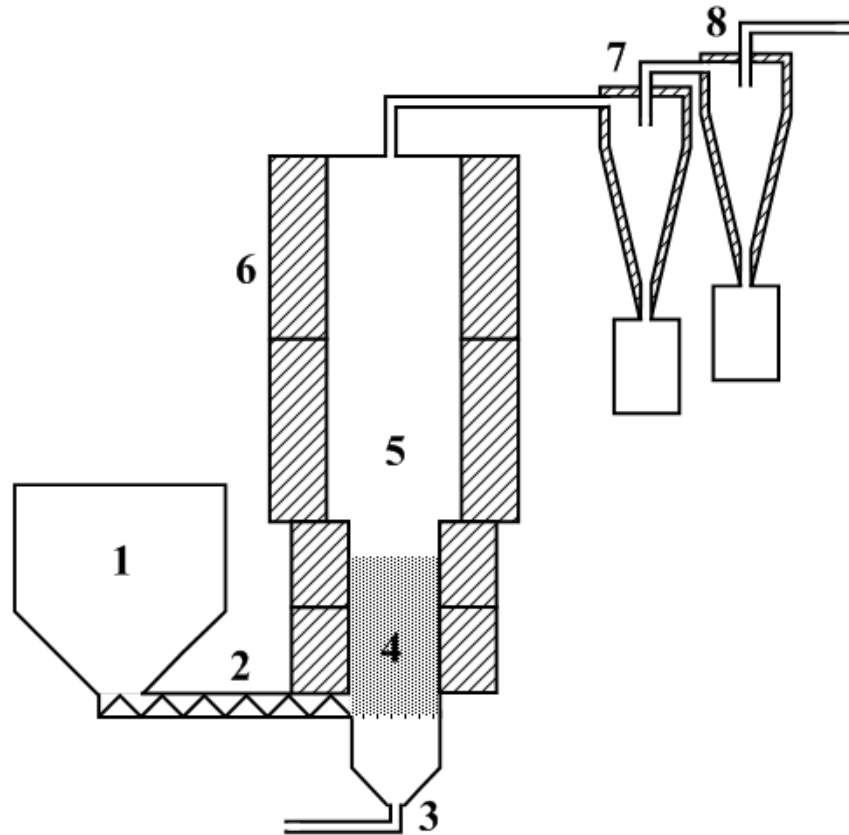
Figure 2: Schematic of fluidized bed gasifier and accessory equipment[2]

Heat loss from the gasifier was regulated with four pairs of Watlow radiant ceramic

fiber guard heaters maintained at 730 °C. Temperature throughout the gasifier was measured

with 8 type K thermocouples: one in the plenum, three in the bed, and four in the freeboard.

Four additional thermocouples measured guard heater surface temperatures as part of the

heater control system. Helium (He) was injected into the main producer gas line above the

gasifier as tracer gas for use in calculation of the total producer gas flow rate. All piping

[2]Components are: biomass hopper (1); injection auger (2); plenum (3); fluidized bed (4); freeboard (5); guard heaters (6); high flow cyclone (7); and high efficiency cyclone (8)

above the gasifier was heat traced and maintained at 450 °C to prevent condensation of water and tar. Char was removed from the gas stream by two particulate cyclones installed in series. The first cyclone was designed for gas streams with high particulate loading of larger particles (d_{p50} = 11.6 μm) and the second was designed for gas streams with lower particulate loading of smaller particles (d_{p50} = 4.2 μm). Based on visual inspection of thimble filters, these two cyclones allowed for the capture of the vast majority of particulate entrained in the gas stream.

After exiting the second cyclone, a small slip stream of producer gas was diverted through a sample line for analysis while the majority of gas was directed into a downdraft combustor where it was mixed with natural gas and air, burned, and then exhausted. A schematic of the sample line is presented in Figure 3. The sample line was comprised of a thimble filter, a tar condenser, glass impingers filled with hydrochloric acid (HCl), steel impingers packed with glass wool insulation, a vacuum pump, a wet test meter (Ritter Instruments, Chicago, IL), and a Varian Model CP-4900 Micro Gas Chromatograph (GC) (Varian, Inc., Palo Alto, CA). The thimble filter was an Advantec 88RH quartz fiber filter (Advantec MFS, Inc., Dublin, CA) designed to remove > 99.9 % of particulate > 0.3 μm. The tar condenser contained a 20 ft coil of 0.375 in santoprene tubing and small canister of glass wool insulation. It was filled with water, placed on a hot plate, and maintained at 102 °C to condense tars inside the santoprene while allowing water to pass through as a vapor following from the protocol described by Xu et al. [28] Two glass impingers arranged in series containing 500 ml of 5% HCl solution and placed in an ice bath served to absorb ammonia from the producer gas stream following the protocol developed by Norton et al.

[29]   Impinger tubes packed with glass wool insulation and chilled in an ice bath served to condense any water in the producer gas stream prior to its entrance to the Micro GC. A vacuum pump was used to pull the slip stream from the main gas line to the Micro GC where it was analyzed for He, N_2, carbon monoxide (CO), carbon dioxide (CO_2), hydrogen (H_2), methane (CH_4), acetylene (C_2H_2), ethylene (C_2H_4), and ethane (C_2H_6).
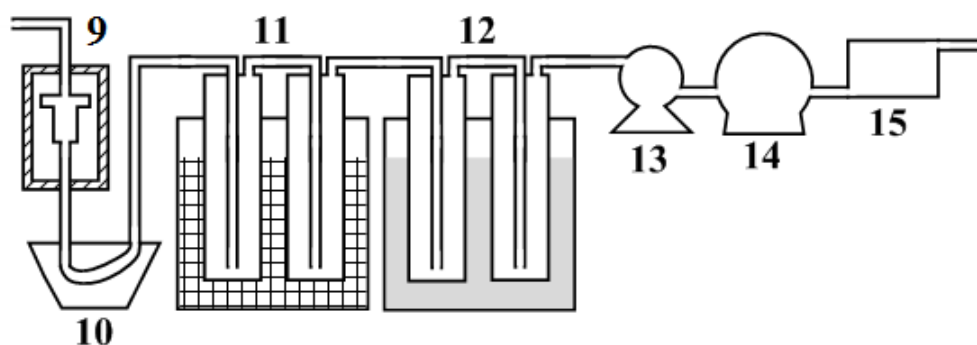
Figure 3: Schematic of gas stream sample line[3]

Target biomass feed rate was 4 kg hr^{-1} (dry basis) although actual feed rate varied due to error associated with the volumetric feed system. Actual feed rate was 4.3±0.7 kg hr^{-1} (mean±SD). Target gasifier temperature was 730 °C and varied slightly due to changes in feed rate. For each experiment, 50.0±0.7 slpm of air was used as a fluidizing agent and 1.00±0.012 slpm of He was used as a tracer gas. Equation 3 shows the calculation of total producer gas flow rate.

---

[3] Components are: heated, thimble filter (9); pressure cooker (10); HCl impingers (11); water impingers (12); vacuum pump (13); wet test meter (14); and gas chromatograph (15)

$$Q_{pg} = \frac{Q_{He} \times (100\% - C_{He})}{C_{He}} \qquad (3)$$

where: Q_{pg} is total producer gas flow rate (slpm)
Q_{He} is He tracer gas flow rate (slpm)
C_{He} is the concentration of He in the producer gas (%)

Char was collected for the duration of each experiment. At the end of each

experiment, char was weighed and samples were collected for elemental analysis. Twice

during each experiment, the gas stream was continuously sampled at a rate of 2 to 3.5 slpm

for 15 minutes. The first sampling period was completed one hour after fuel feed began, and

the second sampling period was completed one hour before the estimated time of burnout.

The same tar condenser assembly was used for both sampling periods to determine the mass

of tar produced during 30 minutes of gasification. A fresh set of impinger tubes was used for

each sample period to determine the amount of ammonia produced during 15 minutes of

gasification. The total amount of tar and ammonia in the gas stream were determined by

scaling up the amount of tar from the tar condenser and ammonia from the HCl impinger

train to the total amount of gas produced, as shown in Equation 4.

$$M_{Produced} = \frac{V_{Total}}{V_{Sampled}} \times M_{Sampled} \qquad (4)$$

where: $M_{Produced}$ is the total mass of tar or NH_3 produced during sample period (kg)
V_{Total} is the volume of gas produced during the sample period (sl)
$V_{Sampled}$ is the volume of gas sampled during the sample period (sl)
$M_{Sampled}$ is the volume of sample collected during the sample period (kg)

The same impinger tubes for water collection were used for both sampling periods.

Gas was sampled every 3.5 min with the Micro GC, supplying four complete sets of gas

composition data for each sample period.

Chemical Analysis

The C and N concentrations of switchgrass, char, and bed media samples were determined by combustion of a 150 mg sample at 950 ºC in a LECO analyzer (Model CHN-2000, LECO Co., St. Joseph, MI). Prior to analysis, biomass was ground to 2 mm using a Thomas-Wiley mill (Model 4, Thomas Scientific, Swedesboro, NJ), ground a second time to 0.5 mm using an Udy Cyclone mill (Udy Co., Ft. Collins, Co). The P and K concentrations of switchgrass biomass, char, and bed media samples were determined using inductively coupled plasma atomic emission spectrometry (ICP-AES) analysis. For this analysis, a 250 mg sample of each of the substances was treated with 5 ml nitric acid at 90 ºC for 30 min, then treated with 3 ml of 30% H_2O_2 and digested for another 90 min at 120 ºC. Following digestion, the solution was diluted to 35 ml with 20% HCl, mixed, filtered and subjected to ICP-AES analysis. Switchgrass biomass was ground prior to ICP-AES analysis following the same protocol described for LECO analysis. The ammonia concentration of HCl impinger contents at the end of each run was determined calorimetrically using a flow-injection analyzer (Latchat Instruments, Milwaukee, WI.).

Mass Balance and Statistical Analysis

The overall experiment was arranged as a randomized complete block design with two nitrogen fertilization treatments (0 and 65 kg ha^{-1}) and four replications. Analysis of variance was conducted using R software (R Development Core Team), with blocks treated as a random factor and fertilization rates treated as a fixed factor [30]. Fertilization-by-year interaction mean squares were used as the error term for assessing differences in mass

balance parameters and elemental recovery rates between the two fertilizer treatments. Variables analyzed according to this approach included feedstock characteristics, overall and element-specific mass balances, and estimates for nutrient recovery in the form of char and liquid ammonia.

Results and Discussion

Feedstock Characteristics

An overview of the switchgrass used in this study is given in Table 2. The table is divided into the two feedstock treatments (0 and 65 kg ha^{-1}). Total switchgrass yield differed with statistical significance, demonstrating that nitrogen fertilization did increase yield. Decreases in dry matter weight between harvest and gasification were due to losses incurred during grinding and transport. Water content between treatments did not differ with statistical significance. The fertilized switchgrass treatment did contain significantly more C, N, and K than the unfertilized treatment; however, P content did not differ between treatments. The largest elemental difference between the two treatments was N content. The higher N content in the fertilized treatment was likely the result of the added nitrogen fertilizer.

Table 2: Yield, moisture and nutrient content of switchgrass[4]

Fertilization (kg ha^{-1})	Dry matter (kg)		H$_2$0 content (g kg^{-1})		Elemental content (g kg^{-1})[a]			
	Harvested	Gasified	Harvested	Gasified	C	N	P	K
0	14.6	13.8	340	52	456.3	2.7	1.1	5.0
65	18.3	17.7	327	46	466.3	4.4	1.2	7.0
LSD[b]	1.1	0.8	NS	NS	4.1	0.2	NS	1.0

[a] Elemental content assessed at the time of gasification [b] LSD significance calculated at $P < 0.05$

Mass and Nutrient Balance

Table 3 summarizes the overall mass balance closure for all 8 experiments. Overall mass balance refers to the percentage of the input streams accounted for by the output streams. Inputs into the system were biomass, biomass moisture, and air. Outputs were biomass nutrients remaining in the bed media, char, tar, ammonia, and gas. The average overall mass balance closure for all 8 experiments was 93±12% (mean ± SD). Overall mass balances for all 8 experiments confirm that the gasifier and accessory equipment accurately accounted for all input and output streams. On average only 0.08% of the total amount of inputs remained in the bed media, 9.48% were converted to char and 1.84% were converted to tar. Ammonia was the only output stream that differed with statistical significance between the unfertilized and fertilized switchgrass treatments. In the unfertilized switchgrass, ammonia accounted for 0.07% of the total system inputs and in the fertilized switchgrass it accounted for 0.12%. This was likely due to the increased N content of the fertilized switchgrass. Gas production accounted for 81.83% of the total system inputs with the majority of this coming in the form of N$_2$, CO, and CO$_2$.

---

[4]Switchgrass was fall harvested when the crop was fertilized with 0 or 65 N kg N ha^{-1} the previous spring

Table 3: Overall mass balance of switchgrass gasification

Material	Balance (% input mass)	
	Mean	SD
Gasifier bed	0.08	0.01
Charcoal	9.48	0.35
Fine	2.13	0.12
Coarse	7.35	0.54
Tar	1.84	0.39
Ammonia[a]	0.07 / 0.12	0.01
Gas	81.83	3.92
N_2	23.03	1.41
CO	23.01	1.08
CO_2	28.03	1.41
H_2	0.34	0.03
CH_4	4.24	0.19
C_2H_2	0.14	0.02
C_2H_4	2.56	0.10
C_2H_6	0.40	0.05
Unaccounted	6.65	4.37

[a] Values are for 0 and 65 kg N ha^{-1} fertilization, respectively, which were significantly different at $P < 0.05$.

A series of box plots depicting overall mass balance closure as well as element-specific mass balance closures are shown in Figure 4. Element-specific mass balances on C, N, P, and K closed to an average of 90%, 56%, 101%, and 71% respectively.
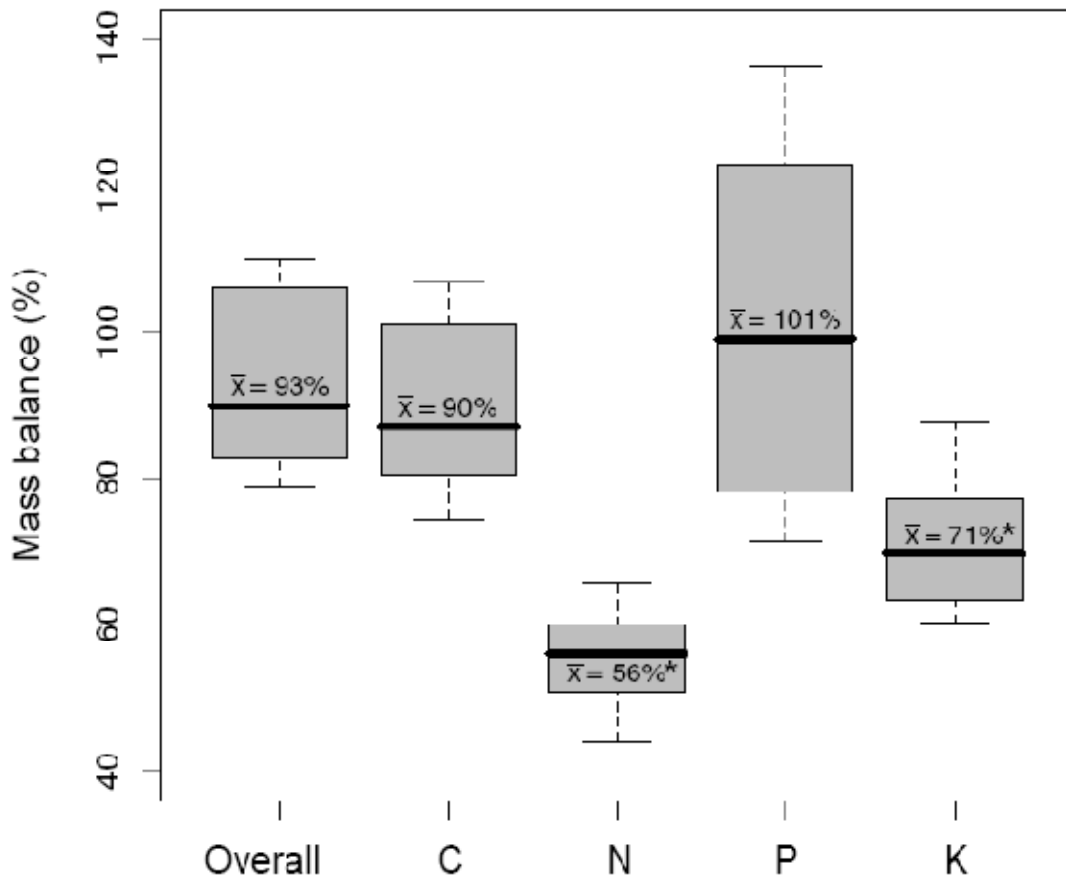
Figure 4: Box plots for the overall and elemental mass balances[5]

Figure 5 shows the same element-specific mass balance closure for C, N, P, and K separated into output stream components. To understand Figure 5, it is important to clarify the difference between nutrient accounting and nutrient recovery. To account for a nutrient in this study referred to tracking the amount of that nutrient exiting in one output stream or another. To recover a nutrient in this study referred to collecting that nutrient in a form that

---

[5]Means followed by an asterisk were significantly different from 100% according to a T-test at $P < 0.05$ (n=4). Mass closures were not affected by feedstock fertilization rate.

could be used as a soil amendment. To further clarify, C was accounted for as coarse char, fine char, gas, and bed media, but only coarse char and fine char signified recovered C. Nitrogen was accounted for as coarse char, fine char, NH_3 in the gas stream, and bed media. All of these forms were considered recovered N with the exception of bed media. Both P and K were accounted for as coarse char, fine char, and bed media, but only coarse char and fine char were considered recovered P and K.
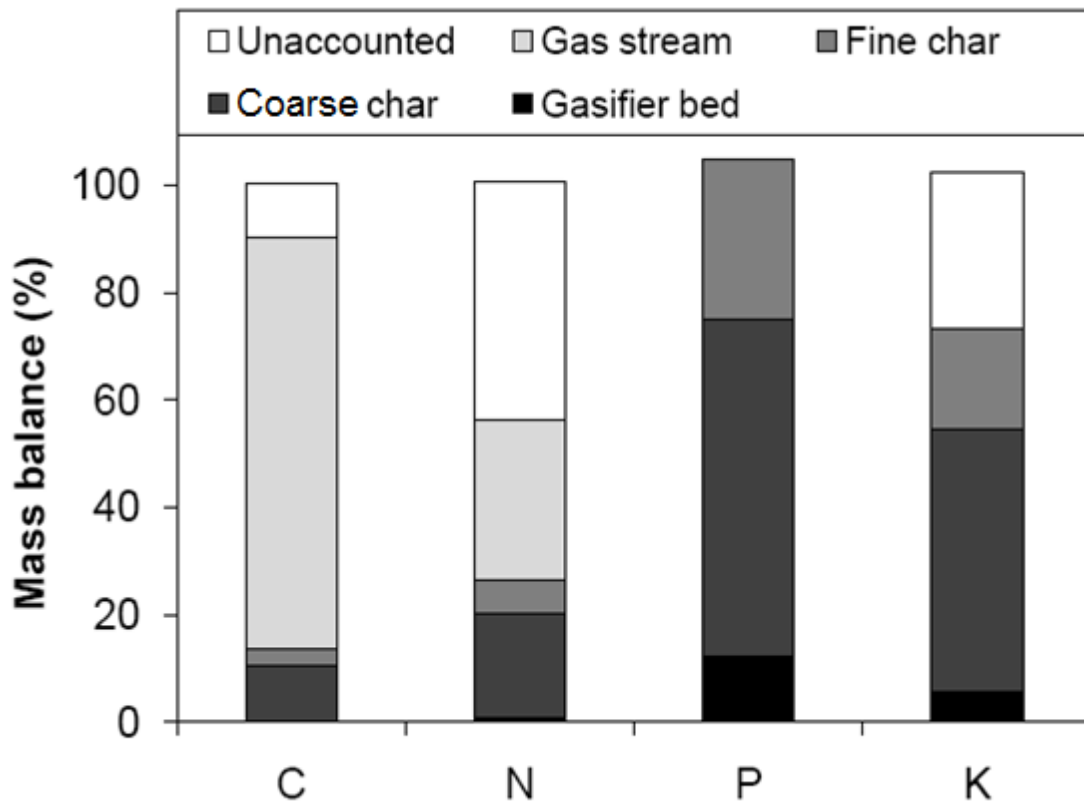
Figure 5: Compartmental mass balances of switchgrass gasification for C, N, P, and K[6]

---

[6]For C, P, and K, mass present in char is potentially recoverable. For N, mass present in char and NH_3 in the gas stream is potentially recoverable.

An average of 76.7% of C in the switchgrass was converted to gas and 10.2% was recovered as coarse char. Only 3.4% of switchgrass C was recovered as fine char. Of the remainder of accounted C, 0.2% remained in the bed media. The high percentage closure on the C-specific mass balances show that C was well accounted for in the system. Carbon conversion as seen in the literature is calculated in Equation 5 [31, 32].

$$CC = \frac{M_{FC} - M_{CC}}{M_{FC}} \qquad (5)$$

where: CC is carbon conversion (%)
  M_{CC} is the mass of carbon in the char (kg)
  M_{FC} is the mass of carbon in the feedstock (kg)

Average carbon conversion for all 8 experiments was 86%. While this meant that the majority of switchgrass C was not captured in a form suitable to be returned to the field for sequestration, it indicated that most of the C was converted to producer gas that could be used to generate heat and power or upgraded to produce fuels and chemicals.

Ammonia in the gas stream accounted for the largest fraction of recovered N with 29.9%. Nitrogen recovered in the form of coarse char accounted for 19.7% of switchgrass N. A total of 6.1% of switchgrass N was recovered as fine char and only 0.6% remained in the bed media. The element-specific mass balance closure on N was less than 100% with statistical significance. This meant that a significant portion of the N in the switchgrass was not recovered (on average 44%). It is possible that a portion of the N was converted to other nitrogen compounds such as hydrogen cyanide (HCN). Lassing et al. [33] found that 35% of fuel N was not found as NH_3 in the gas stream for gasification of miscanthus. This reinforces the conclusion that not all fuel N is converted to NH_3 during gasification. Because NH_3 was

the only form of gaseous N quantified by the sampling procedure it is difficult to speculate on the fate of the unaccounted N.

The majority of switchgrass P was accounted for by char. A total of 62.6% of switchgrass P was recovered as coarse char and 29.9% was recovered as fine char. The remaining 12.4% of switchgrass P remained in the bed media. Of all three biomass nutrients, P showed the greatest average element-specific mass balance closure. The somewhat high spread of element-specific mass balance closures of P as seen in Figure 4 is likely due to the low concentration of P in the switchgrass in conjunction with sample heterogeneity. On average, only 16 g P was fed into the gasifier over the course of an entire experiment compared to 51 g N, 86 g K, and 6148 g C. This small amount of P meant that heterogeneity in the bed media and char samples as well as experimental and analytical error played a more significant role in the closure of the P-specific mass balances than in other element-specific mass balances. This random error associated with the P-specific mass balance closures averaged out over the course of all 8 experiments; however, variability was seen between experiments leading to the large spread seen in Figure 4.

Like P, most of the accounted K was found in the char. A total of 49.2% of switchgrass K was recovered as coarse char and 18.8% of the K was recovered as fine char. Only 5.5% of switchgrass K was retained in the bed media. Unlike P, a significant portion of the switchgrass K fed into the gasifier was not accounted for. This could be explained by a number of reasons. Other experiments that injected KCl into the gasifier revealed that volatilized K often ends up as deposits in gas lines leaving the gasifier [34]. Although the gas lines did not clog during this study, small amounts of K deposition inside the gas lines

could account for a portion of the losses shown in Figure 4. On average, 86 g of switchgrass K was fed into the gasifier over the course of an experiment and 71% of this K was accounted for in output streams. If gas line deposits contained 35 wt% K, as observed in the experiments with injected KCl, 71 g of deposits would need to have formed over the course of each experiment to account for the missing K. While gas line K deposition does not explain all of the missing K, it likely contributed to the lack of closure in the element-specific mass balances of K.

Another possible explanation for the missing K is gas entrainment. Gas entrained K in this context is defined as any K that passed through the cyclones. While gas entrained K was not measured during these experiments, particulate that passed through the cyclones was quantified. On average, a total of 17 g of particulate passed through the cyclones, and was captured in the thimble filter over the course of an entire experiment. Although thimble filter deposits were not analyzed during these experiments, other experiments performed with the same system at similar operating conditions showed thimble filter deposits to be on average 58 wt% K [34]. If thimble filter deposit composition was the same in the case of this study, an average 9.8 g of the total switchgrass K that entered the system would be accounted for in thimble filter deposits. This means that thimble filter deposits could account for 37% of the missing K from this study. Collection of this gas entrained K could significantly increase the total recovery percentage of switchgrass K.

Nutrient Recovery

Table 4 summarizes the recovery of C, N, P, and K as a percentage of the total amount of C, N, P, and K in the switchgrass before gasification. Figure 6 shows the elemental recovery of C, N, P, and K for both treatments of switchgrass on a kg ha^{-1} basis.

Table 4: Elemental recovery as percentage of switchgrass elemental input

| Element | Recovery (% feedstock) | | LSD[a] |
	0 kg ha^{-1}	65 kg ha^{-1}	
C	13.19	13.16	NS
N	52.01	57.81	NS
P	73.37	104.05	25.23
K	60.68	70.51	9.56

[a] LSD significance calculated at $P < 0.05$
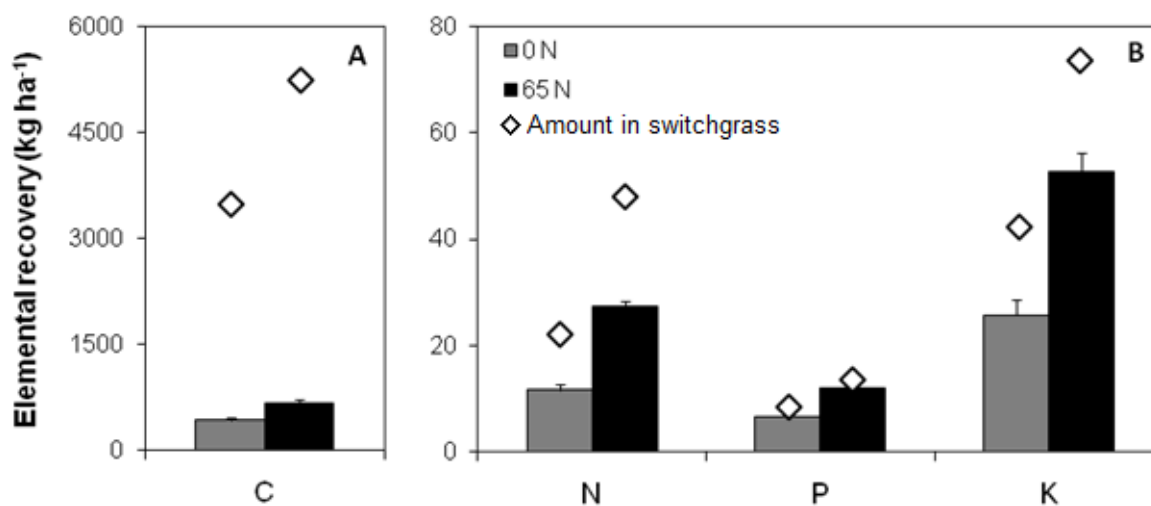
Figure 6: Absolute recovery of C (A) and N, P, and K (B) with either 0 or 65 kg N ha^{-1} [7]

Complete elemental recovery can be broken down into two parts. The first part is C recovery. Table 4 shows that C recovery is independent of nitrogen fertilization. Figure 6

---

[7]Error bars correspond to the standard deviation of elemental recovery (n=4)

shows on an absolute basis that 431 kg ha^{-1} and 681 kg ha^{-1} of C were recovered for the unfertilized and fertilized switchgrass respectively. While C is not a biomass nutrient, Lehmann et al. [3] show that char similar to that produced in this study, can be effectively sequestered in soil. Sequestration of C in this manner allows the field to act as a long term carbon sink. This could potentially create a net negative carbon emission for the entire cycle from field to gasifier and back to field. In this way, no C from the switchgrass is wasted. It is either turned into producer gas for use in the biorefinery or sequestered in the soil, effectively removing CO_2 from the atmosphere.

The second part of elemental recovery is N, P, and K recovery. Management guidelines for the sustainable production of switchgrass as a bioenergy crop indicate that producers should seek to match fertilizer inputs with the quantity of nutrients removed in harvested biomass [35]. Table 4 and Figure 6 clearly show that nutrient recovery can significantly supplement and in some cases completely offset fertilization of switchgrass. In the case of N, nutrient recovery was independent of N fertilization and accounted for 52% to 58% of the total N removed from the field with the switchgrass. Unlike N, a higher recovery percentage of P and K occurred with the fertilized treatment of switchgrass compared to the unfertilized treatment. Phosphorus recovery was 73% of switchgrass P from the unfertilized treatment and 104% of switchgrass P from the fertilized treatment. Potassium recovery was 61% of switchgrass K from the unfertilized treatment and 71% of switchgrass K from the fertilized treatment. This suggests that nitrogen fertilization possibly increased recovery percentage of other nutrients.

These results show that by carefully tracking and recycling nutrients during switchgrass gasification, large percentages of fertilization can be offset. These results bode well for the concept of nutrient recovery in a biorefinery.

Conclusions

Mass balances on an overall basis and an element-specific basis for C, N, P, and K were completed for the gasification of unfertilized and fertilized treatments of switchgrass to determine the feasibility of recovering biomass nutrients during gasification. Element-specific mass balances for C and P show that both elements can be well accounted for in gasification. However, element-specific mass balances on N and K closed to less than 100% with statistical significance. N-specific mass balances could likely be increased by measuring other nitrogen compounds in the gas stream such as HCN, although this would not necessarily increase the amount of recoverable N that could be returned to the field. K-specific mass balances could likely be increased by utilizing a barrier filter to capture gas entrained K passing through the cyclones. This approach could increase K recovery from 66% of the total amount of K in the switchgrass to 77%. On average, 13% of switchgrass C was recovered for sequestration and 55% of N, 89% of P, and 66% of K were recovered in a form suitable to be used as soil amendments.

CHAPTER 4. CARBON CONVERSION DURING GASIFICATION AS A FUNCTION OF POTASSIUM CONTENT OF BIOMASS

A paper to be submitted to *Energy & Fuels*

Patrick M. Meehan[1], Samuel T. Jones[2], and Robert C. Brown[3]

[1]Helped conceive study, developed statistical design, developed methodology, performed experiments, helped perform chemical analysis, performed statistical analysis, and drafted the manuscript. [2]Helped conceive study, developed methodology, advised on experimentation, and edited manuscript. [3]Helped conceive study, developed methodology, and edited manuscript.

Abstract

The goal of this study is to determine the effects of potassium and reaction temperature on carbon conversion during air blown fluidized bed gasification of biomass. Potassium (K) is an effective gasification promoter in coal gasification and co-gasification of coal and biomass. Naturally occurring alkali in biomass is also expected to influence carbon conversion during biomass gasification. A series of 12 experiments was performed to evaluate this hypothesis. A statistical model was developed and analyzed to better understand the results. The results indicate that maximum carbon conversion is achieved when potassium content of biomass is 1.85 wt% K and the gasification temperature is 817 °C. The model also showed that bed temperature was a more important predictor of carbon conversion than was feedstock potassium over the range of operating conditions examined in this study. The observation that carbon conversion decreased above 817 °C was surprising but may be the result of increased devolatilization of K, which would decrease the amount of K in contact with gasifying biomass. The relatively negligible effect of feedstock potassium

content on carbon conversion could be due to the potency of K as a gasification catalyst at concentrations as low as 0.3 wt%.

Introduction

Biomass represents an important source of clean, renewable energy. It is also available in the quantities required to compete in today's energy market [1]. However, to be competitive with fossil fuels, biomass conversion processes must be highly energy efficient. Gasification represents a versatile form of biomass conversion that leads to a producer gas (a mixture of nitrogen (N_2), carbon monoxide (CO), carbon dioxide (CO_2), hydrogen (H_2), methane (CH_4), and short-chain hydrocarbon gases) that can be further converted to liquid transportation fuels and high value chemicals, or simply used as a fuel to generate heat and electricity. Extensive catalysis research has been performed on both primary (in the gasifier) and secondary (downstream of the gasifier) reactors to increase the gasification efficiency [5]. A simpler and less costly method would be to use the inherent properties of the biomass to increase the efficiency of the gasification process.

Different types of biomass contain different amounts of alkali and alkali earth metals such as K, sodium (Na), calcium (Ca), and magnesium (Mg), as seen in Table 5 [6]. Historically the presence of alkali metals during gasification has been viewed as detrimental because they can cause fouling and damage to boiler tubes, turbine blades, and gas clean up equipment [7]. However, more recent research by Brown et al., Godavarty et al., and Sjostrom et al. [8-10] suggest that alkali metals can increase process efficiency. These studies show that alkali increases gasification rate, increases gas production, and decreases

39

char production. It follows then that alkali metals may likely increase the efficiency of

biomass gasification. If correctly understood and implemented, biomass could be selected

for gasification based upon alkali metal content thereby simplifying processing equipment

and saving money.

Table 5: Typical biomass inorganic constituents[8] [6]

Plant organ	Ash	N	C	Al	Ca	Cl	Fe	K	Mg	Na	P	S	Si
Leaves													
Arundo d.	113	15.7	430	461	6167	6986	308	5080	2182	159	803	3511	17232
Cynara c.	117	9.6	417	1781	27802	13143	655	4711	1876	11942	1459	3760	4267
Miscanthus s.	62	6.3	431	595	5262	6701	324	3265	1291	193	396	867	16666
Panicum v. 20	76	7.4	423	543	6922	9490	319	2126	2706	326	774	991	15745
Panicum v. 80	70	8.4	428	435	8182	3617	283	1504	2626	317	578	1048	15036
Fibre s.	81	13.4	424	483	9245	4737	236	8805	3086	195	1246	1105	19736
Sweet s.	82	13.5	425	328	8359	3741	186	11661	2805	189	1273	1099	14858
Mean	86	10.6	425	661	10277	6916	330	5307	2367	1903	933	1769	14791
Stems													
Arundo d.	32	5.2	431	196	968	5608	102	5609	1027	130	320	932	6223
Cynara c.	68	3.0	401	150	12190	18171	79	6467	766	12807	1363	1740	889
Miscanthus s.	19	1.6	439	143	1730	7406	61	3588	857	153	154	337	4531
Panicum v. 20	26	3.0	435	137	1097	13798	86	3555	1020	870	404	464	5345
Panicum v. 80	23	3.3	440	111	1197	4944	83	2628	1171	870	248	443	5301
Fibre s.	41	2.6	409	114	2643	6398	79	12577	1903	193	702	817	5345
Sweet s.	50	4.4	408	152	3446	7199	112	12991	2079	195	804	681	7013
Mean	37	3.3	423	143	3325	9075	86	6774	1260	2174	571	773	4950
Reproductive organs													
Cynara c.	67	14.3	444	106	9960	9863	71	19325	1815	1340	2427	1708	474
Fibre s.	47	13.1	434	242	1824	6252	141	5587	2451	192	2150	1084	10671
Sweet s.	58	14.1	424	218	2417	5129	159	7125	2895	171	2620	1000	14321
Mean	57	13.8	434	189	4734	7081	124	10679	2387	567	2399	1264	8489

Potassium was chosen as the focus of this study because it has been shown to have

the highest interaction with carbon of all alkali metals with the exception of rubidium, which

is not typically found in biomass in appreciable concentrations [36].   A range from 0.3 to 2.7

[8]Ash, N, and C are expressed as g/kg all other elements are expressed as mg/kg

wt% K was selected for this study based upon typical ranges shown in Table 5. This is the first paper to determine the effects of both feedstock potassium and bed temperature on carbon conversion during biomass gasification and track potassium and carbon through a gasifier in an effort to better understand potassium's role in gasification.

Materials and Methods

Fluidized Bed Gasifier

A schematic of the gasifier and ancillary equipment used in these experiments is shown in Figure 7. The gasifier has a bed diameter of 10 cm and a freeboard diameter of 15 cm. The bed was fluidized with 50±0.7 slpm of air metered by a 0 to 150 slpm Alicat mass flow controller (Alicat Scientific Tucson, AZ) and preheated by a Watlow coil heater (Watlow, St. Louis, MO) located in the plenum. This fluidizing gas flow rate was selected to operate the gasifier at a target equivalence ratio (ER) of 0.30. Gasifier temperature was maintained by four pairs of Watlow Clamshell Radiant heaters placed around the reactor. The heaters were operated at temperatures slightly above the gasification temperature, which prevented heat loss from the gasifying biomass, approximating adiabatic reaction conditions. For further information about reactor geometry please refer to Emsick [27].
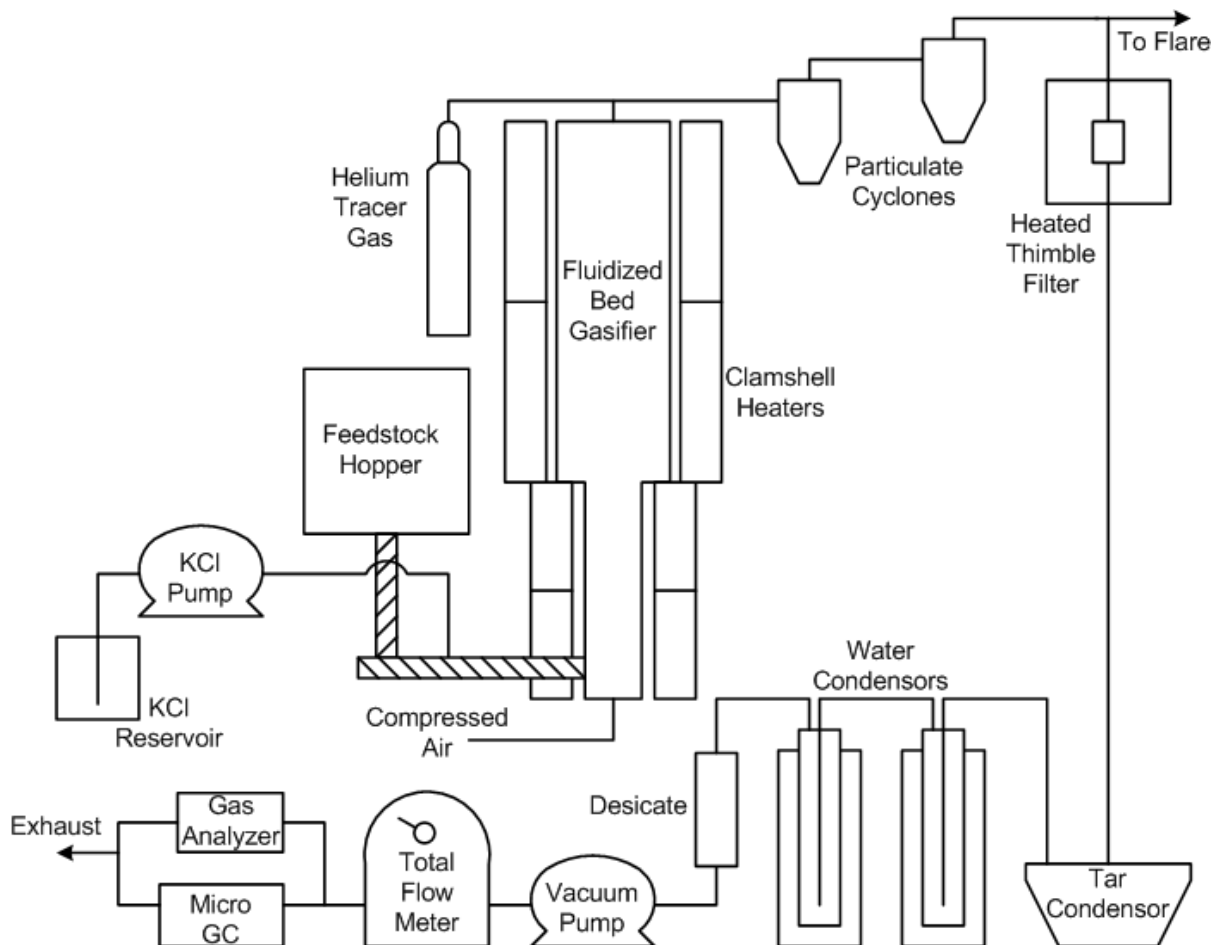
Figure 7: Gasification and ancillary equipment schematic

Biomass and Potassium

Corn fiber was fed at a rate of 1.80 kg hr^{-1} (dry basis) via an auger system. Ultimate

analysis of the corn fiber is shown in Table 6. The corn fiber was a co-product from a wet

mill process. It was a flakey biomass, low in potassium and other inorganic constituents,

with a moisture content of 7.6 to 8.6 wt%. Corn fiber was chosen because its low potassium

content allowed the desired range of feedstock potassium to be simulated with one type of

biomass. In addition, the low concentration of Na in the corn fiber ensured that increases in carbon conversion could be attributed solely to feedstock potassium or bed temperature rather than any other type of biomass alkali.

Table 6: Ultimate analysis of corn fiber

Element	wt% dry basis
C	47.98
H	7.02
O (by diff)	42.00
N	2.00
S	0.23
K	0.19
Na	0.01
Cl	0.03
P	0.02

A Cole-Parmer L/S Digital Console peristaltic pump (Cole-Parmer, Vernon Hills, IL) was used to deliver different amounts of a potassium chloride solution (KCl/H_2O) into the auger where it wetted the corn fiber being fed into the reactor. To measure total gas production, 1.00 ± 0.012 slpm of helium (He) tracer gas was metered by a 0 to 2 slpm Alicat mass flow controller and injected into the gas line directly above the gasifier. After exiting the gasifier, particulate was removed by a pair of cyclones mounted in series.

Sample Line

The gas lines were heat traced to 450 °C to prevent condensation of water and tar. Directly downstream of the cyclones, a slip stream of 2 to 4 slpm was extracted. The balance of the gas stream was mixed with air and combusted before being cooled and exhausted from the laboratory. The slip stream passed through a heated Advantec 88RH quartz fiber thimble filter (Advantec MFS, Inc., Dublin, CA) to remove any trace particulate matter still entrained

in the gas. Tar was condensed in santoprene tubing inside a tar condenser operated at 102 °C

as described in Xu et al [28]. Water was condensed in an impinger train consisting of 2

stainless steel impingers submerged in a 2.5 °C chilled water bath followed by a desiccate

canister filled with Drierite. A vacuum pump was used to pull the gas through the sample

line and a wet test meter (Ritter Instruments, Chicago, IL) measured the total amount of gas

sampled for each experiment. The gas was analyzed with a Varian 4900 Micro gas

chromatograph (GC) (Varian, Inc., Palo Alto, CA) and an infrared non-dispersive continuous

emissions monitor (IR ND CEM) (DeJaye Technologies, Des Moines, IA).

Experimental Procedure

Experiments were initiated by a 1 to 1.5 hr heat up period during which the system

was fluidized and reactor temperature increased with the Watlow heaters. Once the bed

temperature reached 600°C, fuel feed and KCl solution feed were started simultaneously.

Fuel and KCl solution were typically fed for 2.5 to 3.5 hours until bed temperature, bed

carbon loading, and gas composition reached a steady state based on research performed by

Timmer [15]. Bed potassium loading was also assumed to be at steady state after 2.5 to 3.5

hours because the volatilization of potassium is a faster reaction than the gasification

reactions required for carbon to reach steady state. At the end of this transient gasification,

both cyclone catches were changed and gas sampling started. Char collection and gas

sampling were performed for 1 hour. At the end of the sampling period, the fuel feed and

KCl solution feed were turned off and the fluidizing gas was left on, allowing any remaining

fuel or char in the bed to combust. This combustion of remaining fuel and char in the bed is

referred to henceforth as burnout. During burnout, the gas stream was monitored with both

the Micro GC and the IR ND CEM.

The total amount of corn fiber fed was determined by weighing the contents of the

feedstock hopper before and after each experiment. The total amount of potassium fed was

determined by weighing the KCl reservoir before and after every experiment. By varying

feed rate and concentration of the KCl solution, different biomass potassium contents were

simulated.

Total producer gas flow rate was calculated by knowing the flow rate of He tracer gas

into the system, and the concentration of He in the slip stream obtained from the Micro GC

as shown in Equation 6.

$$Q_{pg} = \frac{Q_{He} \times (100\% - C_{He})}{C_{He}} \qquad (6)$$

where: Q_{pg} is total producer gas flow rate (slpm)
          Q_{He} is He tracer gas flow rate (slpm)
          C_{He} is the concentration of He in the producer gas (%)

Because the amount of tar and water collected in the slip stream represented only a

small fraction of the total quantities of these compounds generated in the gasifier, Equation 7

was used to calculate the total amounts.

$$M_{Produced} = \frac{V_{Total}}{V_{Sampled}} \times M_{Sampled} \qquad (7)$$

where: $M_{Produced}$ is the total mass of tar or water produced during sample period (kg)
          V_{Total} is the total amount of gas produced during the sample period (sl)
          $V_{Sampled}$ is the amount of gas sampled during the sample period (sl)
          $M_{Sampled}$ is the amount of sample collected during the sample period (kg)

To determine the amount of carbon in the bed, steady state bed carbon loading was

calculated. Steady state bed carbon loading is defined as the amount of carbon in the bed

media at the time of gas sampling. To calculate this, burnout gas composition was measured

with the IR ND CEM. The analyzer took readings of CO_2 and CO every 5 seconds until the

concentration of CO_2 fell below 1.0 vol% and the concentration of CO reached 0.0 vol%.

Gas flow rate was measured as described before with a He tracer gas. Equation 8 shows how

the total amount of gaseous burnout carbon was calculated. For more information on bed

carbon loading and burnout gas quantification, please refer to Christofides [37].

$$M_C = \left(\frac{Q_{gas} \times dt \times MW_C}{22.4 \frac{L}{mol}}\right) \times (C_{CO} + C_{CO2}) \qquad (8)$$

where: M_C is the mass of carbon in the bed converted to a gas during burnout (g)
 Q_{gas} is the gas flowrate during burnout (slpm)
 dt is the time of the burnout (min)
 MW_C is the molecular weight of carbon (g/mol)
 C_{CO} is the concentration of CO in the gas stream (vol%)
 C_{CO2} is the concentration of CO_2 in the gas stream (vol%)

After every experiment the bed was removed and replaced with fresh bed material

consisting of 1540 g of 300-400 μm silica sand and 660 g crushed limestone to prevent

effects from residual alkali in the bed.

Experimental Design

A 2-D rotatable central composite design of experiments was created based upon 12

total experiments and is depicted in Figure 8. These included four "Factorial" experiments,

four "Alpha" experiments, and four "Centerpoint" experiments. The experimental conditions

are shown in Figure 8. Target conditions for bed temperature were achieved in every

experiment and target conditions for added potassium were achieved to within ±0.14%. The

"Factorial" experiments represented a full factorial of 2 variables, feedstock potassium and

bed temperature, and two levels, 0.6 wt% K or 2.4 wt% K and 700 °C or 850 °C. The

"Alpha" experiments served to expand the experimental range over which conclusions could

be drawn to feedstock potassium contents from 0.3 wt% K to 2.7 wt% K and bed

temperatures from 675 °C to 875 °C. These operating conditions approached but did not

reach conditions at which the system could not reliably operate. The "Centerpoint"

experiments were performed in the middle of the system's operable range. Four experiments

were replicated at the centerpoint condition of 1.5 wt% K and 775 °C to determine the

experimental error in the system. This error was then applied to all other operating

conditions. The experimental error was found to be significantly larger than the instrumental

error. Therefore the experimental error was considered to be the total error.
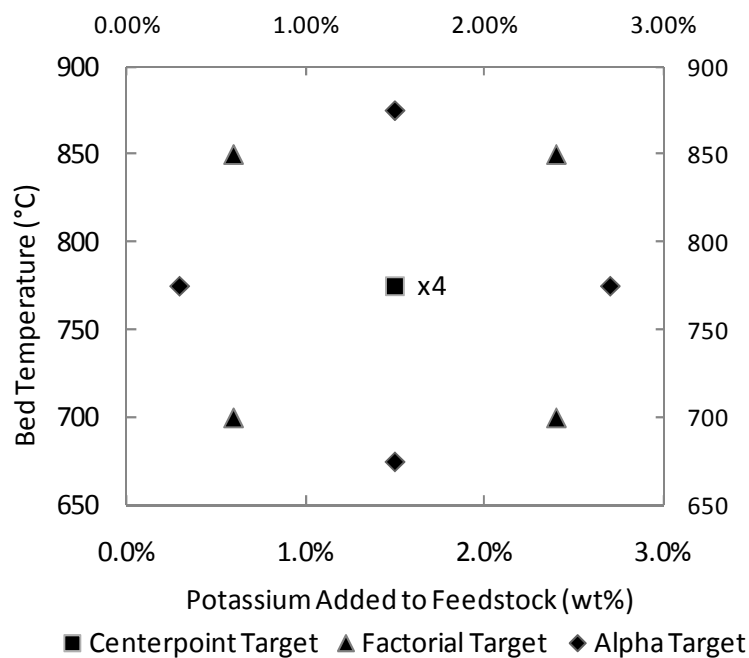
Figure 8: Experimental operating conditions

A comprehensive mass balance was completed for the 1 hr steady state sampling period. It accounted for the total amount of corn fiber, KCl, water, and air entering the system and the total amount of char, tar, water, and gas leaving the system.

Carbon conversion was calculated for each experiment and used as a metric to compare conversion efficiently for the various experimental operating conditions. Carbon conversion is defined in Equation 9 [31, 32].

$$CC = \frac{M_{FC} - M_{CC}}{M_{FC}} \qquad (9)$$

where: CC is carbon conversion (%)
M_{CC} is the mass of carbon in the steady state char (kg)
M_{FC} is the mass of carbon in the steady state feedstock (kg)

Sample Analysis and Model Development

A LECO CHN analyzer (LECO Co., St. Joseph, MI) was used to determine the carbon content of the biomass, bed material, and char from every experiment to allow carbon mass balances to be checked. The total amount of gaseous carbon leaving the bed during burnout was added to the amount of solid carbon remaining in the bed after burnout to calculate the steady state bed carbon loading inside the gasifier. Nitric acid microwave digestions were performed on bed material and char samples as detailed in EPA Method 3051 [38]. The digestions were then analyzed for K using inductively coupled plasma atomic emission spectrometry (ICP-AES) analysis to allow potassium to be tracked through the system.

After data were collected and analyzed, a statistical model was developed using the software package Minitab 15 (Minitab Inc., State College, PA) to investigate the effects of both feedstock potassium and bed temperature on carbon conversion [39].

Results and Discussion

Mass Balance and Exit Stream Composition

Table 7 shows a comparison of gas composition, char and tar loading in the gas stream, and carbon conversion between this research and literature as reported by van der Drift et al., Wander et al., Gil et al., and Li et al. [31, 32, 40, 41] Water content in the gas is not comparable to traditional air blown gasification literature because approximately 450 g hr^{-1} of water was fed into the gasifier with the KCl solution. While the water flow rate into the gasifier was constant for all 12 experiments, the amount of water in the gas stream was elevated as a result. Gas composition, char and tar loading, and carbon conversion from this study compared well with literature values [31, 32, 40, 41].

Table 7: Gas composition comparison to literature

	This study		Literature	
	Low	High	Low	High
Gas (%vol, dry)				
H_2	5.23	14.44	1.80	18.89
N_2	51.06	61.71	41.60	73.68
CH_4	1.71	3.56	1.08	6.20
CO	6.07	14.77	5.34	22.71
CO_2	13.71	20.74	9.00	19.40
C_2H_4	0.64	1.96	0.26	1.15
C_2H_2	0.01	0.10	-	-
C_2H_6	0.07	0.28	0.02	0.26
Metrics (g/m^3)				
Char/Gas	1.04	43.61	0.17	13.10
Tar/Gas	0.90	10.23	0.02	15.10
CC (%)	90.10	99.70	85.20	98.40

A complete data summary for all 12 experiments is presented in Table 8. Char loading in the gas varied from 1.0 to 43.6 g m^{-3}, tar loading varied from 0.9 to 10.2 g m^{-3}, and water loading varied from 84.9 to 282.8 g m^{-3}. Producer gas composition on a dry basis is given for all 12 experiments in Table 9. These data were used to complete comprehensive mass balances for all 12 experiments, the results of which are shown in Figure 9. The average mass balance closure was 101±5.8% (mean±SD). Error in mass balance closure was likely due to measurement error related to the total producer gas flow rate calculation based upon the He tracer gas. Overall, this represents an accurate account of all mass into and out of the system.
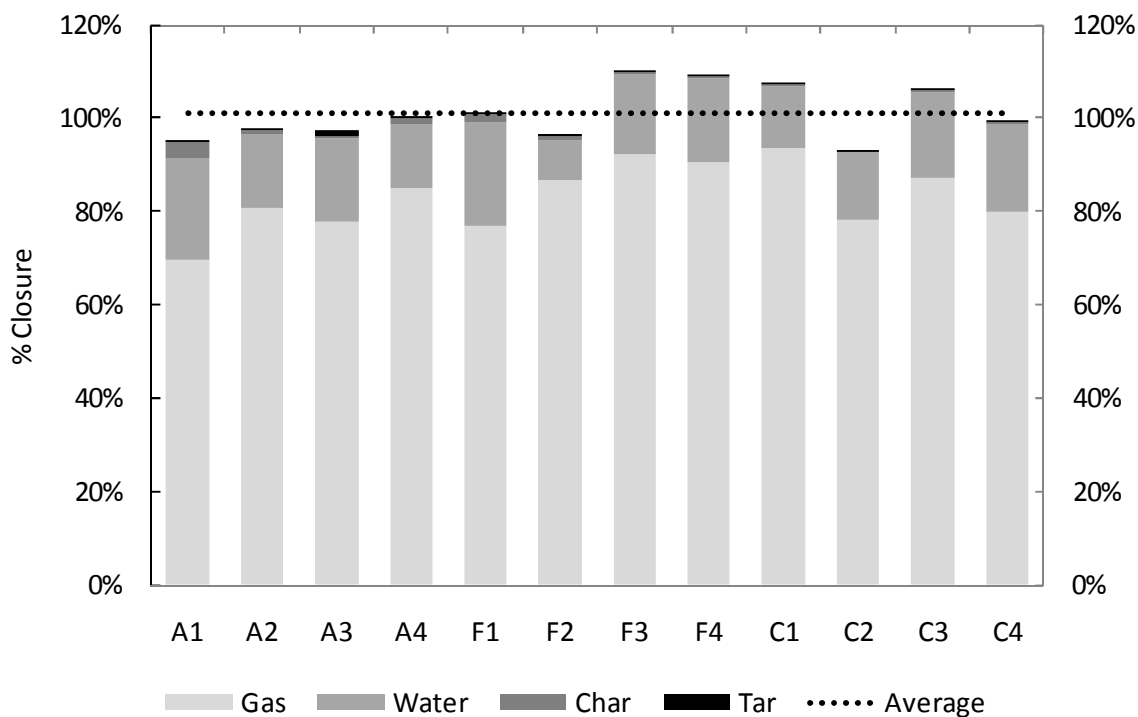
Figure 9: Overall mass balance closure

Table 8: Operating conditions, process inputs, process outputs, and metrics

Operating Conditions	Alpha Experiments				Factorial Experiments				Centerpoint Experiments				Centerpoint Statistics	
	A1	A2	A3	A4	F1	F2	F3	F4	C1	C2	C3	C4	Avg.	Std. Dev.
Temperature	675	875	775	775	700	850	700	850	775	775	775	775	775	0
K %wt added	1.64	1.51	2.69	0.26	0.57	0.58	2.47	2.41	1.54	1.58	1.64	1.56	1.58	0.04
ER	0.33	0.31	0.30	0.29	0.30	0.31	0.32	0.31	0.31	0.32	0.32	0.32	0.32	0.01
Inputs (kg/hr)														
Fuel	1.680	1.813	1.878	1.911	1.838	1.816	1.729	1.817	1.801	1.768	1.728	1.724	1.755	0.037
Air	1.932	1.932	1.932	1.932	1.932	1.932	1.932	1.932	1.932	1.932	1.932	1.932	1.932	0.000
Water	0.473	0.472	0.462	0.513	0.512	0.513	0.473	0.481	0.488	0.495	0.503	0.481	0.492	0.009
KCl	0.045	0.044	0.092	0.000	0.011	0.011	0.076	0.078	0.045	0.046	0.047	0.044	0.045	0.001
Outputs (kg/hr)														
Char	0.138	0.038	0.027	0.053	0.076	0.047	0.005	0.018	0.024	0.011	0.023	0.015	0.018	0.006
Tar	0.020	0.010	0.041	0.009	0.016	0.017	0.004	0.011	0.007	0.007	0.011	0.021	0.012	0.006
Water	0.898	0.670	0.782	0.611	0.947	0.357	0.720	0.784	0.550	0.612	0.768	0.793	0.681	0.118
Gas	2.883	3.449	3.393	3.696	3.310	3.704	3.889	3.894	3.999	3.316	3.676	3.340	3.583	0.322
Metrics (g/m^3)														
Char/Gas	43.6	9.6	6.9	13.0	20.8	11.2	1.0	4.1	5.2	3.3	5.7	4.1	4.6	1.1
Tar/Gas	6.2	2.5	10.2	2.2	4.4	4.1	0.9	2.6	1.7	2.1	2.5	5.6	3.0	1.8
Water/Gas	282.8	167.8	196.5	148.7	259.3	84.9	155.2	182.9	122.6	177.6	186.2	212.4	174.7	37.8

Table 9: Producer gas composition

Gas Concentration (vol%, dry)	Alpha Experiments				Factorial Experiments				Centerpoint Experiments				Centerpoint Statistics	
	A1	A2	A3	A4	F1	F2	F3	F4	C1	C2	C3	C4	Avg.	Std. Dev.
H_2	5.37	12.87	14.44	6.89	5.23	10.97	10.80	8.92	8.68	7.11	8.46	7.80	8.01	0.71
N_2	59.42	51.06	51.72	56.71	60.03	53.08	56.54	54.88	57.64	61.71	56.41	59.69	58.86	2.33
CH_4	3.12	3.22	1.84	3.56	2.74	3.43	1.71	3.33	3.05	2.79	3.23	2.67	2.93	0.25
CO	9.41	11.84	11.20	10.82	10.04	10.62	14.77	9.04	7.90	6.50	9.28	6.07	7.44	1.46
CO_2	18.80	17.42	17.93	17.76	18.27	18.28	13.71	20.39	19.55	17.33	18.90	20.74	19.13	1.42
C_2H_4	1.36	1.74	1.03	1.96	1.51	1.89	0.64	1.65	1.45	1.26	1.70	1.01	1.36	0.29
C_2H_2	0.06	0.10	0.04	0.10	0.08	0.10	0.06	0.07	0.05	0.01	0.05	0.03	0.04	0.02
C_2H_6	0.28	0.07	0.13	0.15	0.24	0.08	0.08	0.07	0.13	0.11	0.17	0.11	0.13	0.03

Bed Potassium and Carbon Loading

Figure 10 shows steady state bed potassium loading as a function of feedstock potassium. As feedstock potassium increased steady state bed potassium loading increased for all bed temperatures. This same conclusion has been reached by Turn et al. and Salo et al. [13, 19]
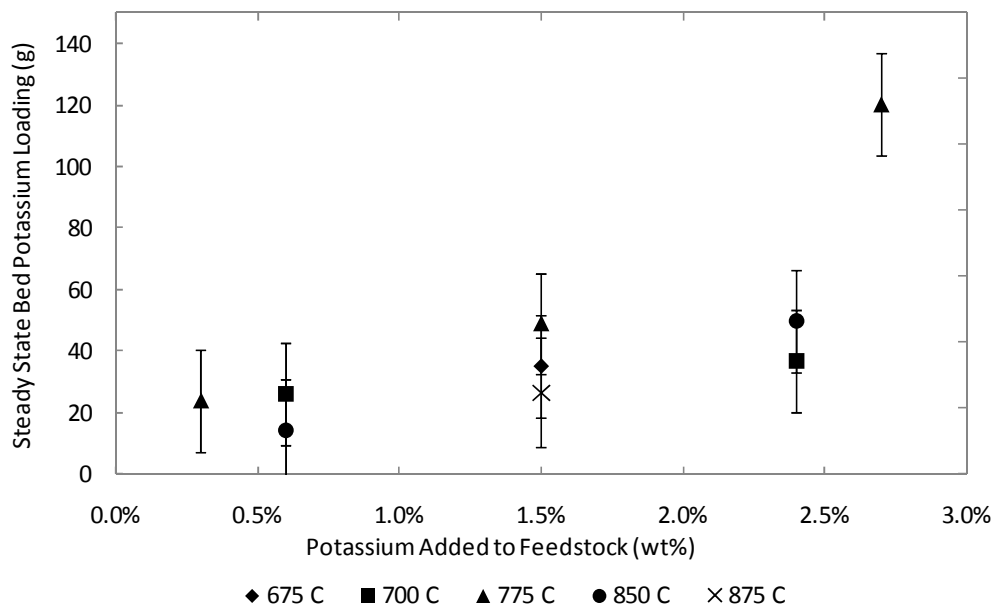
Figure 10: Steady state bed potassium loading as a function of feedstock potassium

Steady state bed carbon loading as a function of feedstock potassium is presented in Figure 11. It is also presented as a function of bed temperature in Figure 12. Figure 11 shows that for a bed temperature of 700 °C, steady state bed carbon loading was proportional to feedstock potassium. It also shows that for a bed temperature of 775 °C, steady state bed carbon loading was unaffected by feedstock potassium for low feedstock potassium contents and proportional to feedstock potassium for high feedstock potassium contents. Figure 12

shows that steady state bed carbon loading was inversely proportional to bed temperature for feedstock potassium content of 2.4 wt% K. Steady state bed carbon loading was independent of feedstock potassium at a bed temperature of 850 °C and independent of bed temperature for feedstock potassium contents from 0.4 to 1.5 wt% K. Figure 12 shows that 426 g of carbon accumulated in the bed when a fuel with a potassium content of 2.4 wt% K was gasified at a bed temperature of 700 °C. This suggests much more carbon was "sequestered" in the bed when a high potassium feedstock was gasified at a low temperature. At these conditions, carbon was not being converted to a gas but was instead being retained in the bed.
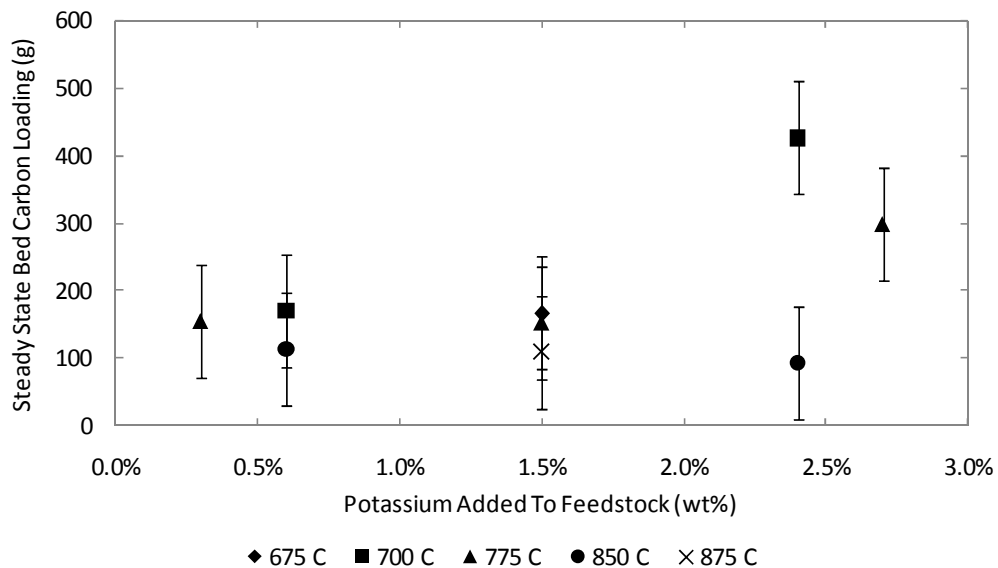
Figure 11: Steady state bed carbon loading as a function of feedstock potassium
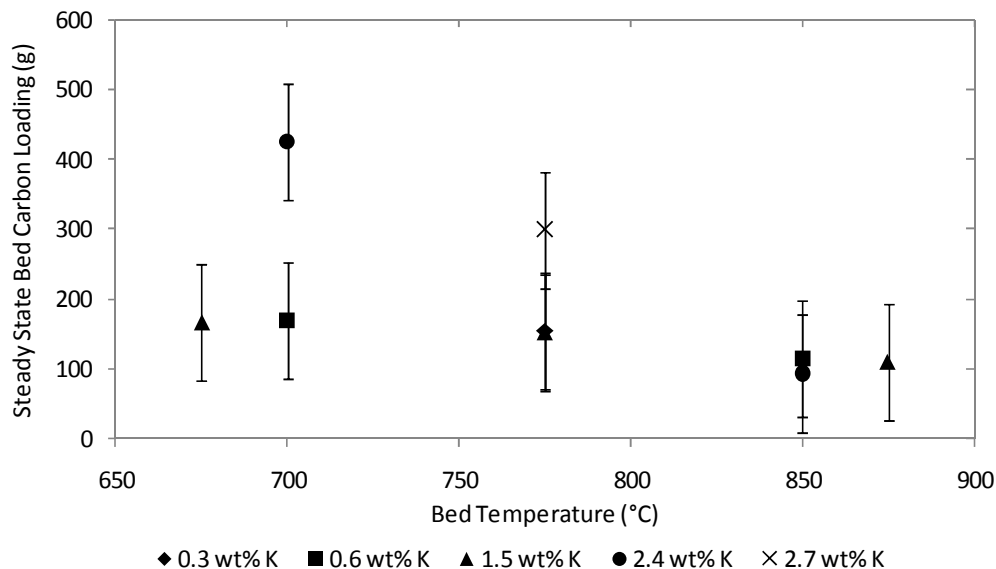
Figure 12: Steady state bed carbon loading as a function of bed temperature

Carbon Conversion

Carbon conversion is plotted as a function of feedstock potassium in Figure 13 and as a function of bed temperature in Figure 14. The average carbon conversion for all 12 experiments was 98.0±2.8% (mean±SD). Figure 13 shows that carbon conversion increased with feedstock potassium content for bed temperatures of 700 °C and 850 °C. It also shows a maximum carbon conversion was attained at 1.5 wt% K for a bed temperature of 775 °C. Figure 14 shows that carbon conversion increased with bed temperature for feedstock potassium content of 0.6 wt% K, and decreased with bed temperature for feedstock potassium content of 2.4 wt% K. The experimental conditions that yielded the maximum carbon conversion were feedstock potassium content of 2.4 wt% K and a bed temperature of 700 °C. These results suggest that carbon conversion was not strictly a monotonic function

of increasing potassium content and bed temperature. Rather, they suggest that a maximum

carbon conversion was reached near the upper range of feedstock potassium content and bed
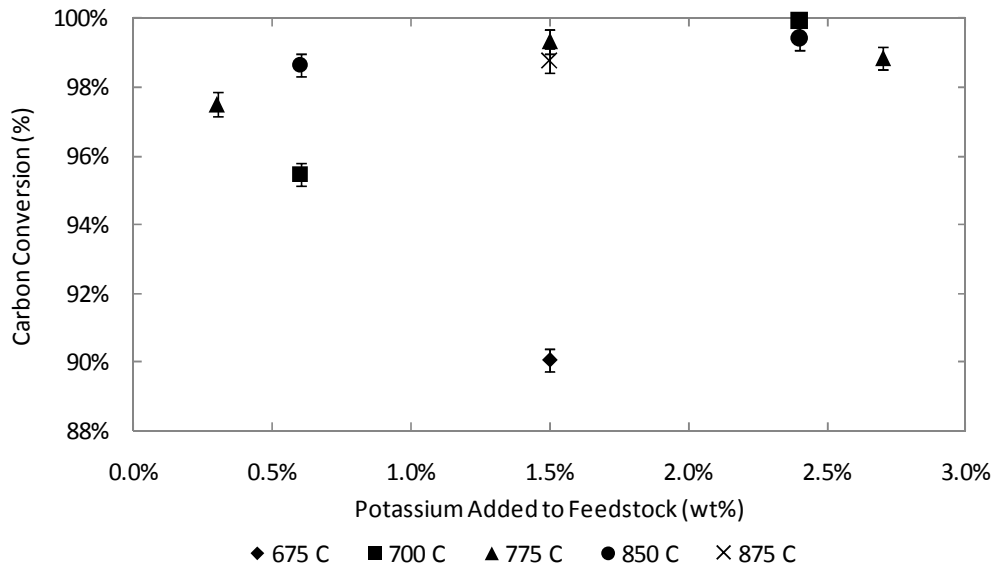
temperature.

Figure 13: Carbon conversion as a function of feedstock potassium
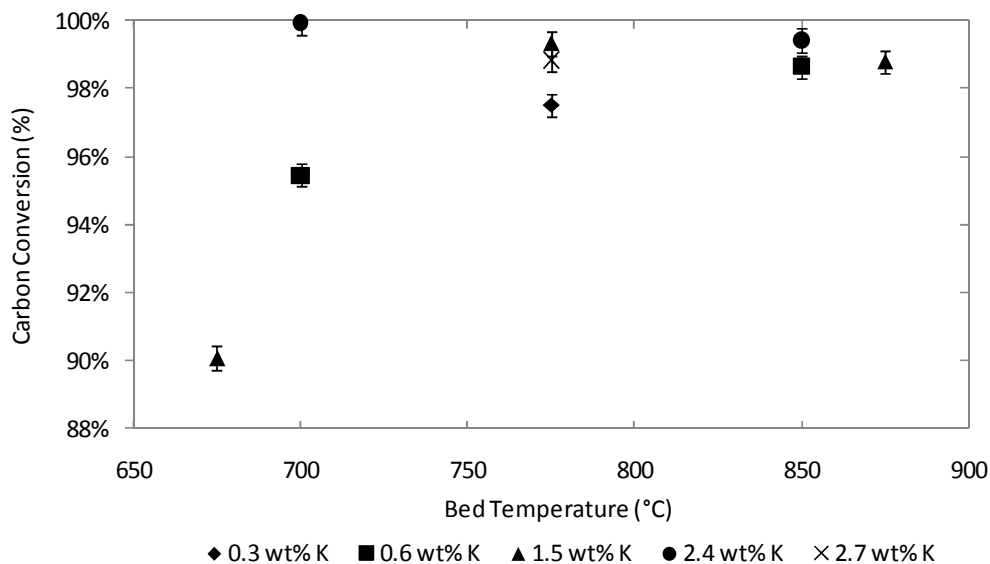
Figure 14: Carbon conversion as a function of bed temperature

Model Development and Analysis

To further investigate this possibility, a statistical model was developed from the experimental data. A full quadratic model was generated using data from all 12 experiments. The generalized equation is shown in Equation 10.

$$CC = C_1 + C_2 \times K + C_3 \times T + C_4 \times K^2 + C_5 \times T^2 + C_6 \times K \times T \qquad (10)$$

where: CC is the carbon conversion (%)
                C_i are model coefficients
                K is feedstock potassium (wt%)
                T is bed temperature in (°C)

The accompanying statistical analysis of the full quadratic model reported that data from the A1 and F3 (as labeled in Table 8) experiments produced unusually high residuals suggesting that these data points represented outliers. The outliers were removed and a

second full quadratic model was generated. Hypothesis testing at $P < 0.05$ concluded that the

interaction effect (the final term in Equation 10) between feedstock potassium and bed

temperature did not affect carbon conversion. This interaction effect was removed and a

third model was generated. Hypothesis testing of the third model showed that every term

was significant at $P < 0.05$. Furthermore, regression analysis concluded that the model fit the

experimental data with an R-squared value of 96.86%. The model equation, R-squared

value, as well as carbon conversion plotted as a function of bed temperature for different

feedstock potassium contents are all shown in Figure 15. The model predicts an increase in

carbon conversion with bed temperature until a maximum carbon conversion is reached

between 775 °C and 850 °C. In addition, it predicts an increase in carbon conversion with

feedstock potassium content until a maximum carbon conversion is reached between 0.6 wt%

K and 2.4 wt% K.
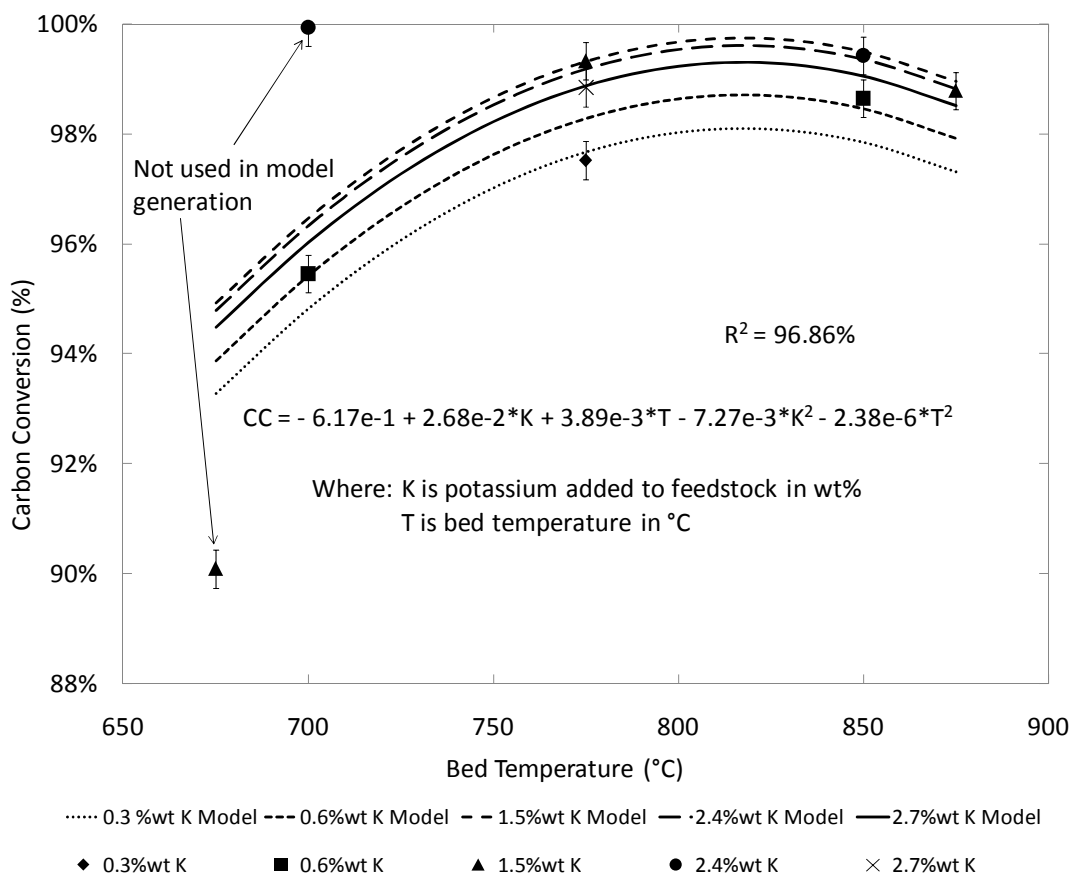
Figure 15: Statistical model of carbon conversion as a function of temperature[9]

To more accurately determine the carbon conversion maximum, a contour plot of the carbon conversion versus bed temperature and feedstock potassium is shown in Figure 16. It shows that maximum carbon conversion of 99.8% is attained for a feedstock potassium content of 1.85 wt% K and a bed temperature of 817 °C. A carbon conversion of > 99% is predicted for feedstock potassium contents ranging from 0.8 to 2.7 wt% K and bed temperatures from 763 to 875 °C. The contours exhibit an elliptical pattern with the longer

---

[9]Five different alkali contents are plotted. The model is based on 10/12 experiments (Data from A1 and F3 experiments was not used in model generation due to high residual values).

elliptical axis being that of feedstock potassium. This means that changing feedstock potassium content has less effect on carbon conversion than changing bed temperature over this range of operating conditions.
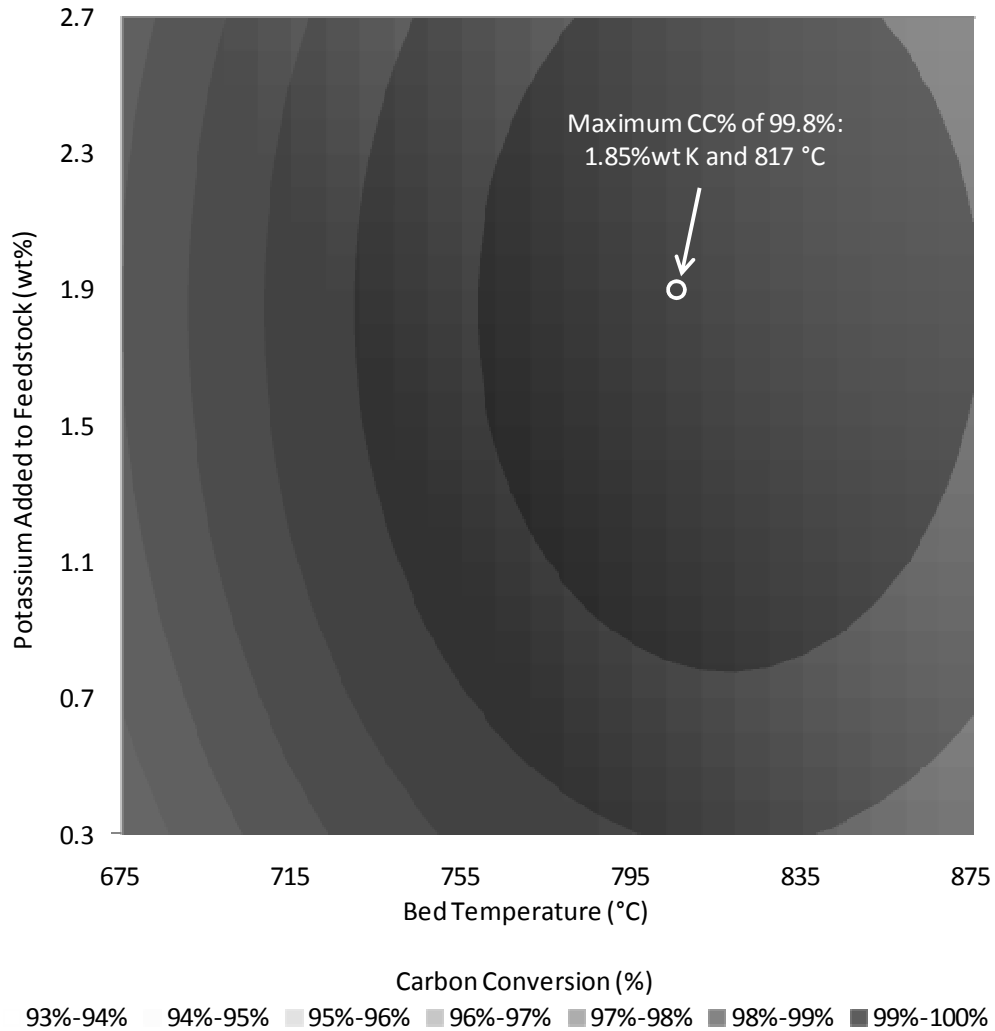
Figure 16: Contour plot of carbon conversion v. feedstock potassium and bed temperature

These small changes in carbon conversion due to feedstock potassium content could be due to the potency of K as a gasification catalyst. If K acts as an effective gasification

catalyst at feedstock potassium contents of 0.3 wt% (the lowest feedstock potassium content used in this study) increasing feedstock potassium above this concentration would do little to increase carbon conversion, as seen in this study. For any fixed bed temperature, increasing feedstock potassium content from 0.3 to 2.7 wt% causes a change in carbon conversion of < 3%. However, for any fixed feedstock potassium content, increasing bed temperature from 675 to 875 °C will cause carbon conversion to change by > 5%. Also, contour lines appear closer together as bed temperature moves away from maximum carbon conversion. This means that as gasification conditions become less ideal, small changes in bed temperature have greater effects on carbon conversion.

The conclusion that carbon conversion does not continue to increase with increasing bed temperature is not necessarily intuitive. To understand this result, the fate of both feedstock carbon and feedstock potassium in the gasifier must be understood. Timmer [15] shows that increasing bed temperature increases carbon conversion. Furthermore, he attributes this increase in carbon conversion to an increased biomass volatile release and concludes that conversion of biomass fixed carbon is independent of bed temperature.

Vaporization is the predominant pathway for K release during gasification as reported by Matsuoka et al. [21] Because increasing bed temperature increases the fraction of gas phase potassium as reported by Salo et al., [19] the amount of feedstock potassium actively in contact with biomass fixed carbon likely decreases as temperature increases. This increase in gas phase K causes a decrease in the effectiveness of K as a gasification catalyst because K must remain in the liquid phase to effectively catalyze gasification reactions according to Chen et al. [42] Therefore, as temperature increases conversion of biomass fixed carbon

likely decreases. When this decrease in fixed carbon conversion as a result of increased temperature exceeds the increase in biomass volatile release as a result of increased temperature, further increases in temperature would cause a net decrease in carbon conversion as predicted by the model developed in this research.

Conclusions

A series of 12 experiments was performed to evaluate the effects of feedstock potassium and bed temperature on carbon conversion in air blown fluidized bed gasification. A statistical model was developed and analyzed to better understand these effects. The model predicted maximum carbon conversion for a feedstock potassium content of 1.85 wt% K and a bed temperature of 817 °C. The model also showed that carbon conversion was affected more by changes in bed temperature than changes in feedstock potassium content over the range of operating conditions used in this study. The conclusion that carbon conversion began to decrease at bed temperatures above 817 °C was attributed to a likely increase in gas phase K at these conditions that would decrease contact between K and biomass fixed carbon and therefore decrease carbon conversion. The small effect of feedstock potassium on carbon conversion over the range of feedstock potassium contents used in this study could be due to the potency of K as a gasification catalyst at concentrations as low as 0.3 wt%.

CHAPTER 5. GENERAL CONCLUSIONS

General Discussion

Mass balances on an overall basis and an element-specific basis for C, N, P, and K were completed for the gasification of unfertilized and fertilized treatments of switchgrass. The goal of the study was to determine the feasibility of recovering biomass nutrients during gasification thus increasing the sustainability of switchgrass as a potential energy crop. Element-specific mass balances for C and P show that both elements can be well accounted for in gasification. However, element-specific mass balances on N and K closed to less than 100% with statistical significance. N-specific mass balances could likely be increased by measuring other nitrogen compounds in the gas stream such as HCN, although this would not necessarily increase the amount of recoverable N that could be returned to the field. K-specific mass balances could likely be increased by utilizing a barrier filter to capture gas entrained K passing through the cyclones. This approach could increase K recovery from 66% of the total amount of K in the switchgrass to 77%. On average, 13% of switchgrass C was recovered for sequestration and 55% of N, 89% of P, and 66% of K were recovered in a form suitable to be used as soil amendments.

A series of 12 experiments was performed to evaluate the effects of feedstock potassium and bed temperature on carbon conversion in air blown fluidized bed gasification of biomass. A statistical model was developed and analyzed to better understand these effects. The model predicted maximum carbon conversion for a feedstock potassium content of 1.85 wt% K and a bed temperature of 817 °C. The model also showed that carbon

conversion was affected more by changes in bed temperature than changes in feedstock potassium content over the range of operating conditions used in this study. The conclusion that carbon conversion decreased at bed temperatures above 817 °C was attributed to a likely increase in gas phase K at these conditions that would decrease contact between K and biomass fixed carbon and therefore decrease carbon conversion. The small effect of feedstock potassium on carbon conversion could be due to the potency of K as a gasification catalyst at concentrations as low as 0.3 wt%.

These two studies represent valuable first steps toward utilizing the inherent properties of biomass nutrients to help develop a sustainable and efficient bioeconomy.

Recommendations for Future Research

To increase understanding of nutrient recovery, similar sets of experiments need to be performed using many different kinds of biomass. This will broaden the scope of the conclusions reached in the study and make the concept of nutrient recovery more valuable to the bioeconomy by determining which energy crops are most sustainable.

To build upon the study of the effects of feedstock potassium and bed temperature on carbon conversion, experiments over a wider range of feedstock potassium contents and bed temperatures need to be performed. These experiments could not be performed in this study due to equipment limitations. However, data over a wider range of variables would allow the statistical model to be expanded, helping to verify or dispute the optimum conditions suitable for maximum carbon conversion found in this study. Furthermore, gasification of various types of biomass with differing potassium contents could serve to add validity to the model.

APPENDIX A: CHAPTER 3 DATA

Table 10: Data summary for all experiments from Chapter 3

Operating Conditions	Unfertilized Switchgrass				Fertilized Switchgrass				Overall Statistics	
	0N1	0N2	0N3	0N4	65N1	65N2	65N3	65N4	Avg.	Std. Dev.
Temperature (°C)	730	730	730	730	730	730	730	730	730	0
Inputs (kg/hr)										
Fuel	4.032	4.823	4.255	3.552	3.637	5.470	3.837	4.950	4.319	0.692
Air	1.932	1.932	1.932	1.932	1.932	1.932	1.932	1.932	1.932	0.000
Water	0.289	0.301	0.323	0.282	0.568	0.334	0.384	0.401	0.360	0.094
Outputs (kg/hr)										
Char	0.526	0.776	0.620	0.558	0.492	0.796	0.610	0.656	0.629	0.110
Tar	0.037	0.280	0.074	0.115	0.052	0.129	0.165	0.135	0.123	0.077
Gas	4.508	6.715	5.225	5.417	4.898	5.179	5.746	5.318	5.376	0.652
Ammonia	0.004	0.005	0.004	0.004	0.008	0.008	0.009	0.008	0.006	0.002
Metrics (g/m3)										
Char/Gas	110.7	109.1	112.1	97.5	95.5	146.8	97.7	119.5	111.1	16.7
Tar/Gas	7.9	39.3	13.3	20.1	10.1	23.7	26.4	24.6	20.7	10.2
Ammonia/Gas	0.9	0.7	0.7	0.8	1.5	1.5	1.5	1.4	1.1	0.4

Table 11: Gas composition summary for all experiments from Chapter 3

Gas Concentration (% dry vol)	Unfertilized Switchgrass				Fertilized Switchgrass				Overall Statistics	
	0N1	0N2	0N3	0N4	65N1	65N2	65N3	65N4	Avg.	Std. Dev.
H2	7.06	8.04	8.10	-	7.83	8.26	10.87	8.65	8.40	1.19
N2	45.65	43.05	43.16	-	43.88	42.89	40.46	38.40	42.50	2.37
CH4	6.34	6.63	6.50	-	5.87	7.03	6.80	7.42	6.66	0.50
CO	17.96	20.75	21.57	-	18.63	21.66	20.41	23.87	20.69	1.98
CO2	16.49	15.69	15.83	-	17.11	15.21	15.77	15.96	16.01	0.61
C2H4	2.14	2.36	2.35	-	2.17	2.37	2.13	2.64	2.31	0.18
C2H2	0.10	0.12	0.12	-	0.12	0.08	0.22	0.13	0.13	0.04
C2H6	0.34	0.35	0.38	-	0.34	0.43	0.13	0.47	0.35	0.11

Table 12: Sample analysis summary for all experiments from Chapter 3

Coarse Char (%wt)	Unfertilized Switchgrass				Fertilized Switchgrass				Overall Statistics	
	0N1	0N2	0N3	0N4	65N1	65N2	65N3	65N4	Avg.	Std. Dev.
C	42.92	41.89	35.27	42.38	37.03	45.27	43.13	42.90	41.35	3.39
N	0.52	0.60	0.46	0.62	0.59	0.74	0.65	0.83	0.63	0.12
P	0.60	0.60	0.73	0.35	0.81	0.87	0.77	0.36	0.64	0.20
K	2.75	2.27	2.58	1.65	3.42	3.52	3.15	2.48	2.73	0.63
Fine Char (%wt)										
C	48.34	45.37	44.88	48.13	45.52	50.16	50.66	53.10	48.27	2.93
N	0.56	0.60	0.57	0.68	0.73	0.81	0.74	0.90	0.70	0.12
P	0.82	1.03	1.02	0.72	1.27	1.12	1.20	1.31	1.06	0.21
K	2.97	3.11	3.47	3.54	4.37	3.51	3.54	4.11	3.58	0.47
Bed Material (%wt)										
C	0.65	0.20	0.29	0.40	0.75	0.58	0.48	0.39	0.47	0.18
N	0.02	0.01	0.01	0.01	0.02	0.01	0.01	0.01	0.01	0.00
P	0.09	0.07	0.05	0.11	0.13	0.11	0.09	0.10	0.09	0.03
K	0.25	0.21	0.19	0.23	0.22	0.21	0.19	0.19	0.21	0.02

APPENDIX B. CHAPTER 4 DATA

Table 13: Data summary for all experiments from Chapter 4

Operating Conditions	Alpha Experiments				Factorial Experiments				Centerpoint Experiments				Centerpoint Statistics	
	A1	A2	A3	A4	F1	F2	F3	F4	C1	C2	C3	C4	Avg.	Std. Dev.
Temperature (°C)	675	875	775	775	700	850	700	850	775	775	775	775	775	0
K added (%wt)	1.89	1.77	2.94	0.53	0.84	0.84	2.73	2.66	1.80	1.84	1.90	1.82	1.84	0.04
ER	0.33	0.31	0.30	0.29	0.30	0.31	0.32	0.31	0.31	0.32	0.32	0.32	0.32	0.01
Inputs (kg/hr)														
Fuel	1.680	1.813	1.878	1.911	1.838	1.816	1.729	1.817	1.801	1.768	1.728	1.724	1.755	0.037
Air	1.932	1.932	1.932	1.932	1.932	1.932	1.932	1.932	1.932	1.932	1.932	1.932	1.932	0.000
Water	0.473	0.472	0.462	0.513	0.512	0.513	0.473	0.481	0.488	0.495	0.503	0.481	0.492	0.009
KCl	0.045	0.044	0.092	0.000	0.011	0.011	0.076	0.078	0.045	0.046	0.047	0.044	0.045	0.001
Outputs (kg/hr)														
Char	0.138	0.038	0.027	0.053	0.076	0.047	0.005	0.018	0.024	0.011	0.023	0.015	0.018	0.006
Tar	0.020	0.010	0.041	0.009	0.016	0.017	0.004	0.011	0.007	0.007	0.011	0.021	0.012	0.006
Water	0.898	0.670	0.782	0.611	0.947	0.357	0.720	0.784	0.550	0.612	0.768	0.793	0.681	0.118
Gas	2.883	3.449	3.393	3.696	3.310	3.704	3.889	3.894	3.999	3.316	3.676	3.340	3.583	0.322
Metrics (g/m3)														
Char/Gas	43.6	9.6	6.9	13.0	20.8	11.2	1.0	4.1	5.2	3.3	5.7	4.1	4.6	1.1
Tar/Gas	6.2	2.5	10.2	2.2	4.4	4.1	0.9	2.6	1.7	2.1	2.5	5.6	3.0	1.8
Water/Gas	282.8	167.8	196.5	148.7	259.3	84.9	155.2	182.9	122.6	177.6	186.2	212.4	174.7	37.8

Table 14: Gas composition summary for all experiments from Chapter 4

Gas Concentration (% dry vol)	Alpha Experiments				Factorial Experiments				Centerpoint Experiments				Centerpoint Statistics	
	A1	A2	A3	A4	F1	F2	F3	F4	C1	C2	C3	C4	Avg.	Std. Dev.
H2	5.37	12.87	14.44	6.89	5.23	10.97	10.80	8.92	8.68	7.11	8.46	7.80	8.01	0.71
N2	59.42	51.06	51.72	56.71	60.03	53.08	56.54	54.88	57.64	61.71	56.41	59.69	58.86	2.33
CH4	3.12	3.22	1.84	3.56	2.74	3.43	1.71	3.33	3.05	2.79	3.23	2.67	2.93	0.25
CO	9.41	11.84	11.20	10.82	10.04	10.62	14.77	9.04	7.90	6.50	9.28	6.07	7.44	1.46
CO2	18.80	17.42	17.93	17.76	18.27	18.28	13.71	20.39	19.55	17.33	18.90	20.74	19.13	1.42
C2H4	1.36	1.74	1.03	1.96	1.51	1.89	0.64	1.65	1.45	1.26	1.70	1.01	1.36	0.29
C2H2	0.06	0.10	0.04	0.10	0.08	0.10	0.06	0.07	0.05	0.01	0.05	0.03	0.04	0.02
C2H6	0.28	0.07	0.13	0.15	0.24	0.08	0.08	0.07	0.13	0.11	0.17	0.11	0.13	0.03

Table 15: Sample analysis summary for all experiments from Chapter 4

Gas Concentration (% dry vol)	Alpha Experiments				Factorial Experiments				Centerpoint Experiments				Centerpoint Statistics	
	A1	A2	A3	A4	F1	F2	F3	F4	C1	C2	C3	C4	Avg.	Std. Dev.
H2	5.37	12.87	14.44	6.89	5.23	10.97	10.80	8.92	8.68	7.11	8.46	7.80	8.01	0.71
N2	59.42	51.06	51.72	56.71	60.03	53.08	56.54	54.88	57.64	61.71	56.41	59.69	58.86	2.33
CH4	3.12	3.22	1.84	3.56	2.74	3.43	1.71	3.33	3.05	2.79	3.23	2.67	2.93	0.25
CO	9.41	11.84	11.20	10.82	10.04	10.62	14.77	9.04	7.90	6.50	9.28	6.07	7.44	1.46
CO2	18.80	17.42	17.93	17.76	18.27	18.28	13.71	20.39	19.55	17.33	18.90	20.74	19.13	1.42
C2H4	1.36	1.74	1.03	1.96	1.51	1.89	0.64	1.65	1.45	1.26	1.70	1.01	1.36	0.29
C2H2	0.06	0.10	0.04	0.10	0.08	0.10	0.06	0.07	0.05	0.01	0.05	0.03	0.04	0.02
C2H6	0.28	0.07	0.13	0.15	0.24	0.08	0.08	0.07	0.13	0.11	0.17	0.11	0.13	0.03

Table 16: Summary of Minitab output for statistical model used in Chapter 4

Response Surface Regression: CarbonConversion versus Alkali, Temperature
The analysis was done using coded units.

Estimated Regression Coefficients fo Carbon Conversion

Term	Coef	SE Coef	T	P
Constant	0.9932	0.0015	665.6130	0.0000
Alkali	0.0050	0.0014	3.5700	0.0160
Temperature	0.0151	0.0019	8.0440	0.0000
Alkali*Alkali	-0.0073	0.0017	-4.3780	0.0070
Temperature*Temperature	-0.0134	0.0019	-6.9850	0.0010

S	0.0030
R-Sq	96.86%
PRESS	0.0006
R-Sq(pred)	57.59%
R-Sq(adj)	94.36%

Analysis of Variance for Carbon Conversion

Source	DF	Seq SS	Adj SS	Adj MS	F	P
Regression	4	0.0014	0.0014	0.0003	38.6100	0.0010
Linear	2	0.0008	0.0010	0.0005	55.7000	0.0000
Square	2	0.0006	0.0006	0.0003	35.0400	0.0010
Residual Error	5	0.0000	0.0000	0.0000		
Lack-of-Fit	2	0.0000	0.0000	0.0000	0.4100	0.6940
Pure Error	3	0.0000	0.0000	0.0000		
Total	9	0.0014				

Estimated Regression Coefficients for CarbonConversion using data in uncoded units

Term	Coef
Constant	-6.17E-01
Alkali	2.68E-02
Temperature	3.89E-03
Alkali*Alkali	-7.27E-03
Temperature*Temperature	-2.38E-06

APPENDIX C. CYCLONE DESIGN

Constants and Properties

$$St_{50.HE} := 1.17 \cdot 10^{-4}$$

$$St_{50.HR} := .006$$

$$\rho_{g.HE} := .3368 \frac{kg}{m^3}$$

$$\rho_{g.HR} := \rho_{g.HE}$$

$$\delta P_{HE} := .3 psi$$

$$\delta P_{HR} := .05 psi$$

$$Q_{HE} := 1.8 \cdot 50 \cdot \left(\frac{1000}{298}\right) \frac{L}{min}$$

$$Q_{HR} := Q_{HE}$$

$$\mu_{g.HE} := 399.9 \cdot 10^{-7} N \cdot \frac{s}{m^2}$$

$$\mu_{g.HR} := \mu_{g.HE}$$

$$\rho_{p.HE} := 400 \frac{kg}{m^3}$$

$$\rho_{p.HR} := \rho_{p.HE}$$

$$T_{HE} := 1000 K$$

$$T_{HR} := T_{HE}$$

$$um := 10^{-6} m$$

Density and viscosity of gas stream are taken as Nitrogen at 1000 K.

Design Equations (Brown)

$$Eu_{HE} := \sqrt{\frac{12}{St_{50.HE}}}$$

$$Eu_{HR} := \sqrt{\frac{12}{St_{50.HR}}}$$

$$U_{HE} := \sqrt{\frac{(2 \delta P_{HE})}{(Eu_{HE} \cdot \rho_{g.HE})}}$$

$$U_{HR} := \sqrt{\frac{(2 \delta P_{HR})}{(Eu_{HR} \cdot \rho_{g.HR})}}$$

$$D_{c.HE} := \sqrt{\frac{(4 Q_{HE})}{(\pi \cdot U_{HE})}}$$

$$D_{c.HR} := \sqrt{\frac{(4 Q_{HR})}{(\pi \cdot U_{HR})}}$$

$$d_{50.HE} := \sqrt{\frac{(18 \cdot \mu_{g.HE} \cdot D_{c.HE} \cdot St_{50.HE})}{(\rho_{p.HE} \cdot U_{HE})}}$$

$$d_{50.HR} := \sqrt{\frac{(18 \cdot \mu_{g.HR} \cdot D_{c.HR} \cdot St_{50.HR})}{(\rho_{p.HR} \cdot U_{HR})}}$$

Results (Brown)

$Eu_{HE} = 320.256$ $Eu_{HR} = 44.721$

$U_{HE} = 6.193\dfrac{m}{s}$ $U_{HR} = 6.766\dfrac{m}{s}$

$D_{c.HE} = 0.032m$ $D_{c.HR} = 0.031m$

$d_{50.HE} = 1.046 \times 10^{-6}\,m$ $d_{50.HR} = 7.008 \times 10^{-6}\,m$

$$
\begin{pmatrix} A_{HE} \\ B_{HE} \\ C_{HE} \\ E_{HE} \\ F_{HE} \\ L_{HE} \\ K_{HE} \\ M_{HE} \end{pmatrix} := \begin{pmatrix} 4 \\ 2.5 \\ 1.5 \\ .375 \\ .5 \\ .2 \\ .5 \\ .5 \end{pmatrix} \cdot D_{c.HE}
\qquad
\begin{pmatrix} A_{HR} \\ B_{HR} \\ C_{HR} \\ E_{HR} \\ F_{HR} \\ L_{HR} \\ K_{HR} \\ M_{HR} \end{pmatrix} := \begin{pmatrix} 4 \\ 2.5 \\ 1.5 \\ .375 \\ .875 \\ .375 \\ .75 \\ .75 \end{pmatrix} \cdot D_{c.HR}
$$

$$
\begin{pmatrix} A_{HE} \\ B_{HE} \\ C_{HE} \\ E_{HE} \\ F_{HE} \\ L_{HE} \\ K_{HE} \\ M_{HE} \end{pmatrix} = \begin{pmatrix} 5.066 \\ 3.166 \\ 1.9 \\ 0.475 \\ 0.633 \\ 0.253 \\ 0.633 \\ 0.633 \end{pmatrix} in
\qquad
\begin{pmatrix} A_{HR} \\ B_{HR} \\ C_{HR} \\ E_{HR} \\ F_{HR} \\ L_{HR} \\ K_{HR} \\ M_{HR} \end{pmatrix} = \begin{pmatrix} 4.847 \\ 3.029 \\ 1.818 \\ 0.454 \\ 1.06 \\ 0.454 \\ 0.909 \\ 0.909 \end{pmatrix} in
$$

Diagram (Brown)
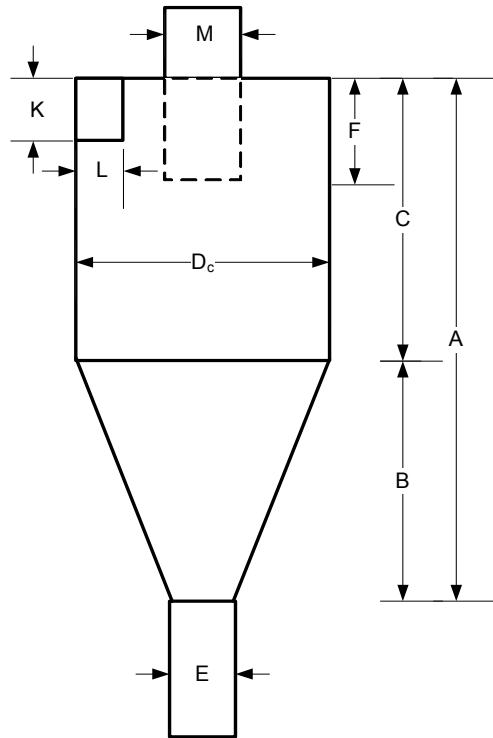
Noemenclature (Hoffmann and Stein)

Dimensional Noemenclature Conversion

$$
\begin{pmatrix} a_{HE} \\ b_{HE} \\ D_{HE} \\ D_{x.HE} \\ D_{d.HE} \\ S_{HE} \\ H_{HE} \\ H_{c.HE} \end{pmatrix} := \begin{pmatrix} K_{HE} \\ L_{HE} \\ D_{c.HE} \\ M_{HE} \\ E_{HE} \\ F_{HE} \\ A_{HE} \\ B_{HE} \end{pmatrix}
\qquad
\begin{pmatrix} a_{HR} \\ b_{HR} \\ D_{HR} \\ D_{x.HR} \\ D_{d.HR} \\ S_{HR} \\ H_{HR} \\ H_{c.HR} \end{pmatrix} := \begin{pmatrix} K_{HR} \\ L_{HR} \\ D_{c.HR} \\ M_{HR} \\ E_{HR} \\ F_{HR} \\ A_{HR} \\ B_{HR} \end{pmatrix}
$$

$$
\begin{pmatrix} a_{HE} \\ b_{HE} \\ D_{HE} \\ D_{x.HE} \\ D_{d.HE} \\ S_{HE} \\ H_{HE} \\ H_{c.HE} \end{pmatrix} = \begin{pmatrix} 0.633 \\ 0.253 \\ 1.267 \\ 0.633 \\ 0.475 \\ 0.633 \\ 5.066 \\ 3.166 \end{pmatrix} \text{in}
\qquad
\begin{pmatrix} a_{HR} \\ b_{HR} \\ D_{HR} \\ D_{x.HR} \\ D_{d.HR} \\ S_{HR} \\ H_{HR} \\ H_{c.HR} \end{pmatrix} = \begin{pmatrix} 0.909 \\ 0.454 \\ 1.212 \\ 0.909 \\ 0.454 \\ 1.06 \\ 4.847 \\ 3.029 \end{pmatrix} \text{in}
$$

Diagram (Hoffmann and Stein)
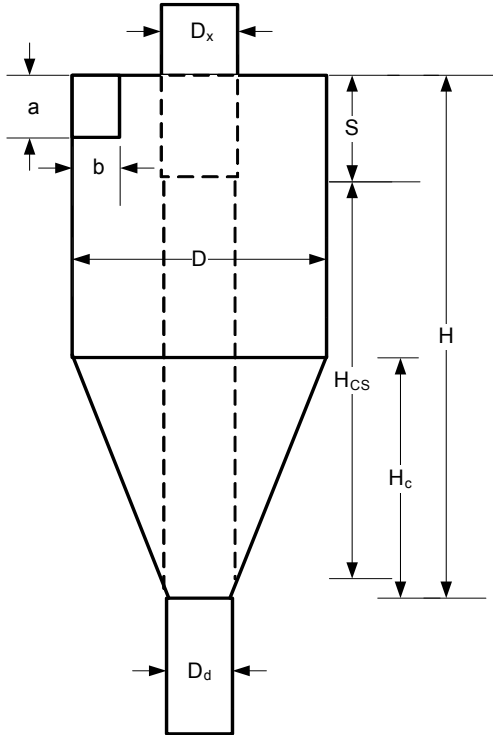
Design Equations (Hoffmann and Stein)

Radii and Velocities (Hoffmann and Stein)

$$R_{HE} := \frac{D_{HE}}{2} \qquad\qquad R_{HR} := \frac{D_{HR}}{2}$$

$$R_{x.HE} := \frac{D_{x.HE}}{2} \qquad\qquad R_{x.HR} := \frac{D_{x.HR}}{2}$$

$$R_{d.HE} := \frac{D_{d.HE}}{2} \qquad\qquad R_{d.HR} := \frac{D_{d.HR}}{2}$$

$$v_{in.HE} := \frac{Q_{HE}}{\left(a_{HE} \cdot b_{HE}\right)} \qquad\qquad v_{in.HR} := \frac{Q_{HR}}{\left(a_{HR} \cdot b_{HR}\right)}$$

$$R_{in.HE} := R_{HE} - \frac{b_{HE}}{2} \qquad\qquad R_{in.HR} := R_{HR} - \frac{b_{HR}}{2}$$

Imaginary Cylinder Surface Height (Hoffmann and Stein)

$$H_{CS.HE} := \left(H_{HE} - S_{HE}\right) - H_{c.HE} \cdot \frac{\left(R_{x.HE} - R_{d.HE}\right)}{\left(R_{HE} - R_{d.HE}\right)} \qquad H_{CS.HE} = 3.8\,\text{in}$$

$$H_{CS.HR} := \left(H_{HR} - S_{HR}\right) - H_{c.HR} \cdot \frac{\left(R_{x.HR} - R_{d.HR}\right)}{\left(R_{HR} - R_{d.HR}\right)} \qquad H_{CS.HR} = 1.969\,\text{in}$$

Velocities and Constriction Coeffecients (Hoffmann and Stein)

$$v_{r.CS.HE} := \frac{Q_{HE}}{\left(\pi \cdot D_{x.HE} H_{CS.HE}\right)} \qquad\qquad v_{r.CS.HR} := \frac{Q_{HR}}{\left(\pi \cdot D_{x.HR} H_{CS.HR}\right)}$$

$$\alpha_{HE} := 1 - 0.4 \left(\frac{b_{HE}}{R_{HE}}\right)^{.5} \qquad\qquad \alpha_{HR} := 1 - 0.4 \left(\frac{b_{HR}}{R_{HR}}\right)^{.5}$$

$$v_{\theta.w.HE} := \frac{\left(v_{in.HE} R_{in.HE}\right)}{\alpha_{HE} \cdot R_{HE}} \qquad\qquad v_{\theta.w.HR} := \frac{\left(v_{in.HR} \cdot R_{in.HR}\right)}{\alpha_{HR} \cdot R_{HR}}$$

Particle Loading and Friction Factor (Hoffmann and Stein)

$$m_{g.HE} := Q_{HE} \cdot \rho_{g.HE} \qquad\qquad m_{g.HR} := Q_{HE} \cdot \rho_{g.HE}$$

$$m_{g.HE} = 6.103 \frac{kg}{hr} \qquad\qquad m_{g.HR} = 6.103 \frac{kg}{hr}$$

$$m_{char.HR} := .5 \frac{kg}{hr}$$

Assuming a capture of ~0.3-0.4 kg/hr with the current cyclone which is operating at 75% effeciency, and the new high flow rate cyclone will capture ~90% of the total char.

$$m_{char.HE} := 0.1 m_{char.HR}$$

$$c_{o.HE} := \frac{m_{char.HE}}{m_{g.HE}} \qquad\qquad c_{o.HR} := \frac{m_{char.HR}}{m_{g.HR}}$$

$$f_{HE} := 0.005 \left[1 + 3 \cdot \left(c_{o.HE} \right)^{.5} \right] \qquad\qquad f_{HR} := 0.005 \left[1 + 3 \cdot \left(c_{o.HR} \right)^{.5} \right]$$

Tangential Cylinder Surface Velocity (Hoffmann and Stein)

$$v_{\theta.CS.HE} := \frac{\left[v_{\theta.w.HE} \left(\frac{R_{HE}}{R_{x.HE}} \right) \right]}{1 + \frac{\left(H_{CS.HE} \cdot R_{HE} \cdot \pi \cdot 8 f_{HE} \cdot v_{\theta.w.HE} \right)}{Q_{HE}}}$$
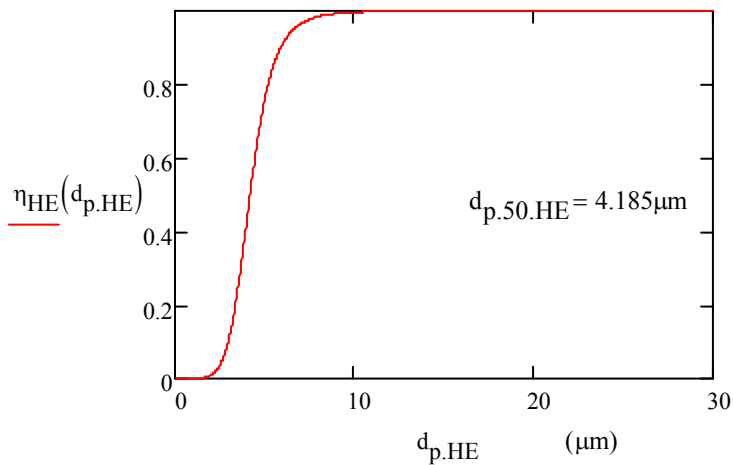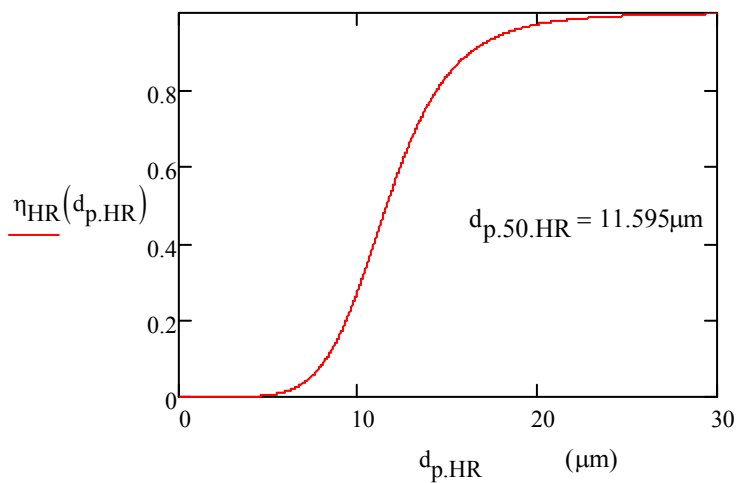
$$v_{\theta.CS.HR} := \frac{\left[v_{\theta.w.HR} \cdot \left(\frac{R_{HR}}{R_{x.HR}} \right) \right]}{1 + \frac{\left(H_{CS.HR} \cdot R_{HR} \cdot \pi \cdot 8 f_{HR} \cdot v_{\theta.w.HR} \right)}{Q_{HR}}}$$

50% Cut Diameters/Separation Effeciencies (Hoffmann and Stein)

$$d_{p.50.HE} := \left[\frac{\left(v_{r.CS.HE} \cdot 9 \cdot \mu_{g.HE} \cdot D_{x.HE}\right)}{\rho_{p.HE} \cdot v_{\theta.CS.HE}^2}\right]^{.5} \qquad d_{p.50.HR} := \left[\frac{\left(v_{r.CS.HR} \cdot 9 \cdot \mu_{g.HR} \cdot D_{x.HR}\right)}{\rho_{p.HR} \cdot v_{\theta.CS.HR}^2}\right]^{.5}$$

$$\eta_{HE}(d_{p.HE}) := \frac{1}{1 + \left(\dfrac{d_{p.50.HE} \cdot 1 \cdot 10^6}{d_{p.HE}}\right)^{6.4}} \qquad \eta_{HR}(d_{p.HR}) := \frac{1}{1 + \left(\dfrac{d_{p.50.HR} \cdot 1 \cdot 10^6}{d_{p.HR}}\right)^{6.4}}$$

Dirgo and Leith Separation Curves

$d_{p.50.HR} = 11.595 \mu m$

$d_{p.50.HE} = 4.185 \mu m$

Pressure Drop Calculation as Check (Hoffmann and Stein)

Shepard and Lapple Analysis

$$\delta P_{check.HE} := \left(\frac{1}{2}\right) \cdot \rho_{g.HE} \cdot v_{in.HE}^2 \cdot \frac{\left(16 \cdot a_{HE} \cdot b_{HE}\right)}{D_{x.HE}^2}$$

$$\delta P_{check.HR} := \left(\frac{1}{2}\right) \cdot \rho_{g.HR} \cdot v_{in.HR}^2 \cdot \frac{\left(16 \cdot a_{HR} \cdot b_{HR}\right)}{D_{x.HR}^2}$$

$\delta P_{check.HE} = 0.37 \, psi$ $\qquad$ $\delta P_{check.HR} = 0.07 \, psi$

$\delta P_{HE} = 0.3 \, psi$ $\qquad$ $\delta P_{HR} = 0.05 \, psi$

SECTION A-A
SCALE 1 : 1.3

| DWG. NO. HR Cyclone Body | | REV. 1 |
| SCALE 1:1.3 | MATERIAL: STAINLESS STEEL | SHEET 2 OF 6 |

Item#	Description
1	HR Cyclone
2	HR Cyclone Entrance
3	1/2" SS Socket Weld Standard Flange
4	1/2" SS Blind Standard Flange, Hole Drilled to 0.65"OD
5	1" SS Blind Standard Flange, Hole Drilled to 1.11"OD

TRUE R0.56

TRUE R0.42

1/2" Standard Pipe can be welded here to accommodate flange.

All connections are welded. If some holes need to be slightly over drilled to accomadate other parts that is fine.

TRUE R0.33

HR Cyclone Assembly Exploded

SECTION A-A
SCALE 1 : 1.3

HE Cyclone Body

Item#	Description
6	HE Cyclone
7	HE Cyclone Entrance
8	1" SS Socket Weld Standard Flange
9	1/2" SS Blind Standard Flange, Hole Drilled to 0.68"OD
10	1" SS Blind Standard Flange, Hole Drilled to 0.83"OD

TRUE R0.42

⑩

⑦

⑥

⑧

1" Standard Pipe can be welded here to accommodate flange.

TRUE R0.66

⑨

TRUE R0.34

All connections are welded. If some holes need to be slightly over drilled to accommodate other parts that is fine.

DWG. NO.
HE Cyclone Assembly Exploded   REV. 1
SCALE:1:2   MATERIAL: STAINLESS STEEL   SHEET 4 OF 6

BIBLIOGRAPHY

1. Perlack, R.D., Wright, L.L., Turhollow, A.F., Graham, R.L., Stokes, B.J., and Erbach, D.C., *Biomass as Feedstock for a Bioenergy and Bioproducts Industry: The Technical Feasibility of a Billion-Ton Annual Supply.* 2005, Oak Ridge National Laboratory: Oak Ridge.

2. Anex, R.P., Lynd, L.R., Laser, M.S., Heggenstaller, A.H., and Liebman, M., *Potential for Enhanced Nutrient Cycling through Coupling of Agricultural and Bioenergy Systems.* Crop Sci, 2007. **47**(4): p. 1327-1335.

3. Lehmann, J., Gaunt, J., and Rondon, M., *Bio-Char Sequestration in Terrestrial Ecosystems – a Review.* Mitigation and Adaptation Strategies for Global Change, 2006. **11**(2): p. 395-419.

4. Day, D., Evans, R.J., Lee, J.W., and Reicosky, D., *Economical Co2, Sox, and Nox Capture from Fossil-Fuel Utilization with Combined Renewable Hydrogen Production and Large-Scale Carbon Sequestration.* Energy, 2005. **30**(14): p. 2558-2579.

5. Corella, J., Toledo, J.M., and Padilla, R., *Olivine or Dolomite as in-Bed Additive in Biomass Gasification with Air in a Fluidized Bed: Which Is Better?* Energy Fuels, 2004. **18**(3): p. 713-720.

6. Monti, A., Di Virgilio, N., and Venturi, G., *Mineral Composition and Ash Content of Six Major Energy Crops.* Biomass and Bioenergy, 2008. **32**(3): p. 216-223.

7. French, R.J., Dayton, D.C., and Milne, T.A., *The Direct Observation of Alkali Vapor Species in Biomass Combustion and Gasification*, in *Other Information: PBD: Jan 1994*. 1994. p. Size: 89 p.

8. Brown, R.C., Liu, Q., and Norton, G., *Catalytic Effects Observed During the Co-Gasification of Coal and Switchgrass.* Biomass and Bioenergy, 2000. **18**(6): p. 499-506.

9. Godavarty, A. and Agarwal, A., *Distribution and Catalytic Activity of Eutectic Salts in Steam Gasification of Coal.* Energy Fuels, 2000. **14**(3): p. 558-565.

10. Sjostrom, K., Chen, G., Yu, Q., Brage, C., and Rosen, C., *Promoted Reactivity of Char in Co-Gasification of Biomass and Coal: Synergies in the Thermochemical Process.* Fuel, 1999. **78**(10): p. 1189-1194.

11. Brown, R.C., *Biorenewable Resources: Engineering New Products from Agriculture.* 2003, Ames: Blackwell Publishing.

12. Narvaez, I., Orio, A., Aznar, M.P., and Corella, J., *Biomass Gasification with Air in an Atmospheric Bubbling Fluidized Bed. Effect of Six Operational Variables on the Quality of the Produced Raw Gas.* Ind. Eng. Chem. Res., 1996. **35**(7): p. 2110-2120.

13. Turn, S.Q., Kinoshita, C.M., Ishimura, D.M., and Zhou, J., *The Fate of Inorganic Constituents of Biomass in Fluidized Bed Gasification.* Fuel, 1998. **77**(3): p. 135-146.

14. Devi, L., Ptasinski, K.J., and Janssen, F.J.J.G., *A Review of the Primary Measures for Tar Elimination in Biomass Gasification Processes.* Biomass and Bioenergy, 2003. **24**(2): p. 125-140.

15. Timmer, K.J., *Carbon Conversion in Bubbling Fluidized Bed Biomass Gasification*, in *Mechanical Engineering; Biorenewable Resources and Technology*. 2007, Iowa State University: Ames.

16. Thompson, D. and Argent, B.B., *The Mobilisation of Sodium and Potassium During Coal Combustion and Gasification.* Fuel, 1999. **78**(14): p. 1679-1689.

17. Garcia-Garcia, A., Illan-Gomez, M.J., Linares-Solano, A., and Salinas-Martinez de Lecea, C., *Nox Reduction by Potassium-Containing Coal Briquettes. Effect of Preparation Procedure and Potassium Content.* Energy Fuels, 2002. **16**(3): p. 569-574.

18. Dayton, D.C., French, R.J., and Milne, T.A., *Direct Observation of Alkali Vapor Release During Biomass Combustion and Gasification. 1. Application of Molecular Beam/Mass Spectrometry to Switchgrass Combustion.* Energy Fuels, 1995. **9**(5): p. 855-865.

19. Salo, K. and Mojtahedi, W., *Fate of Alkali and Trace Metals in Biomass Gasification.* Biomass and Bioenergy, 1998. **15**(3): p. 263-267.

20. Gabra, M., Nordin, A., Ohman, M., and Kjellstrom, B., *Alkali Retention/Separation During Bagasse Gasification: A Comparison between a Fluidised Bed and a Cyclone Gasifier.* Biomass and Bioenergy, 2001. **21**(6): p. 461-476.

21. Matsuoka, K., Yamashita, T., Kuramoto, K., Suzuki, Y., Takaya, A., and Tomita, A., *Transformation of Alkali and Alkaline Earth Metals in Low Rank Coal During Gasification.* Fuel, 2008. **87**(6): p. 885-893.

22. Argent, B.B. and Thompson, D., *Thermodynamic Equilibrium Study of Trace Element Mobilisation under Air Blown Gasification Conditions.* Fuel, 2002. **81**(1): p. 75-89.

23. Kitsuka, T., Bayarsaikhan, B., Sonoyama, N., Hosokai, S., Li, C.Z., Norinaga, K., and Hayashi, J.i., *Behavior of Inherent Metallic Species as a Crucial Factor for Kinetics of Steam Gasification of Char from Coal Pyrolysis.* Energy Fuels, 2007. **21**(2): p. 387-394.

24. Mojtahedi, W., Kurkela, E., and Nieminen, M., *Release of Sodium and Potassium in the Pfb Gasification of Peat* Journal of the Institute of Energy, 1990. **63**: p. 95-100.

25. Basu, P., *Combustion and Gasification in Fluidized Beds*. 2006, Boca Raton: CRC Press.

26. Fernando, S., Adhikari, S., Chandrapal, C., and Murali, N., *Biorefineries:&Nbsp; Current Status, Challenges, and Future Direction.* Energy & Fuels, 2006. **20**(4): p. 1727-1737.

27. Emsick, N., *Switchgrass Derived Producer Gas as a Reburn Fuel*, in *Mechanical Engineering*. 2004, Iowa State University: Ames.

28. Xu, M., Brown, R.C., Norton, G., and Smeenk, J., *Comparison of a Solvent-Free Tar Quantification Method to the International Energy Agency's Tar Measurement Protocol.* Energy Fuels, 2005. **19**(6): p. 2509-2513.

29. Norton, G.A. and Brown, R.C., *Wet Chemical Method for Determining Levels of Ammonia in Syngas from a Biomass Gasifier.* Energy Fuels, 2005. **19**(2): p. 618-624.

30. *R: A Language and Environment for Statistical Computing*. 2008, R Foundation for Statistical Computing: Vienna.

31. van der Drift, A., van Doorn, J., and Vermeulen, J.W., *Ten Residual Biomass Fuels for Circulating Fluidized-Bed Gasification.* Biomass and Bioenergy, 2001. **20**(1): p. 45-56.

32. Wander, P.R., Altafini, C.R., and Barreto, R.M., *Assessment of a Small Sawdust Gasification Unit.* Biomass and Bioenergy, 2004. **27**(5): p. 467-476.

33. Lassing, K., Olsson, E., and Waldheim, L., *Laboratory Analyses and Tests and Calculations: Study Performed within the Framework of the Extended Joule-Iia Programme of Cec Dg Xii Project "Energy from Biomass: An Assessment of Two Promising Systems for Energy Production".* Termiska Processer AB, 1995.

34. Meehan, P., *Quantification of Gas Entrained Potassium.* 2009, Iowa State University: Ames.

35. Parrish, D.J. and Fike, J.H., *The Biology and Agronomy of Switchgrass for Biofuels*, in *Critical Reviews in Plant Sciences*. 2005, Taylor & Francis Ltd. p. 423-459.

36. Suzuki, T., Ohme, H., and Watanabe, Y., *Alkali Metal Catalyzed Carbon Dioxide Gasification of Carbon.* Energy Fuels, 1992. **6**(4): p. 343-351.

37. Christofides, N.J., *Determining Char Burning and Sulfur Sorption Rates from Dynamic Analysis of Carbon Dioxide and Sulfur Dioxide Profiles*, in *Mechanical Engineering*. 1993, Iowa State University: Ames.

38. Kingston, H.M., *Microwave Assisted Acid Digestion of Sediments, Sludges, Soils, and Oils*, E.P. Agency, Editor. 1994, Duquesne University: Pittsburgh.

39. Minitab, *Minitab 15.* 2007, Minitab: State College.

40. Gil, J., Corella, J., Aznar, M.P., and Caballero, M.A., *Biomass Gasification in Atmospheric and Bubbling Fluidized Bed: Effect of the Type of Gasifying Agent on the Product Distribution.* Biomass and Bioenergy, 1999. **17**(5): p. 389-403.

41. Li, X.T., Grace, J.R., Lim, C.J., Watkinson, A.P., Chen, H.P., and Kim, J.R., *Biomass Gasification in a Circulating Fluidized Bed.* Biomass and Bioenergy, 2004. **26**(2): p. 171-193.

42. Chen, S.G. and Yang, R.T., *Unified Mechanism of Alkali and Alkaline Earth Catalyzed Gasification Reactions of Carbon by Co2 and H2o.* Energy & Fuels, 1997. **11**(2): p. 421-427.

ACKNOWLEDGEMENTS

First and foremost I would like to express my gratitude and thanks to Dr. Brown who provided me with an environment in which to perform this research over the past two years. Thanks to his guidance and support, I have been able to take my academic career to the next level and learn about much more than just gasification.

I thank Dr. Heindel for introducing me to Dr. Brown and piquing my interest in graduate school. Thank you to Dr. Raman for introducing me to the bioeconomy through his teaching. I would also like to thank both of them for serving on my committee.

I would like to extend many thanks to the CSET administrative staff who make our lives as graduate students so much easier and enjoyable. I am especially grateful to Diane Love and Becky Staedtler who have saved me countless times by always knowing what do.

I cannot forget the CSET technical staff whose expertise has simplified my life and saved me time more often than I can recall. Dr. Jones has been an invaluable resource on every topic of graduate school from the class room to the laboratory. Without him I most surely would not have been able to solve all of the problems that I did. I would also like to thank Patrick Johnston and Doug Bull for their company in the gasification lab and extensive advice.

Support from fellow graduate students has been most helpful throughout this experience. Whether it was suggestions on experimental methods, help with computer programs, or just empathy for difficulties encountered in the lab, their help has been extremely valuable. While the research group has grown to a size too numerous to name, I thank you all.

Finally, I would like to thank my friends and family for their continued patience and support. My parents, Jim and Ann Meehan, have often offered an old solution to a new problem from their experiences in graduate school and life. And lastly I would like to thank my fiancée, Liz Bainbridge. Without a doubt I would not have been able to survive without having Liz to talk to and provide me with encouragement and fresh, optimistic perspectives on what seemed to me to be impossible problems.